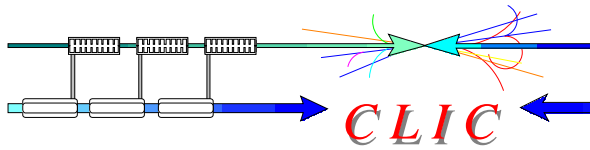


# Comprehensive Analysis of High Gradient RF Test Results and New RF Constraint

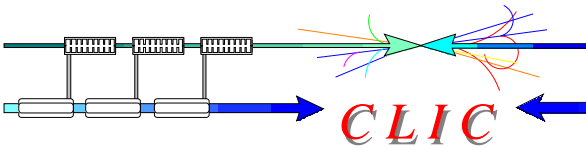
May, 2008  
Alexej Grudiev



## Acknowledgements



- Walter Wuensch
- Sergio Calatroni
- Chris Adolphsen
- Steffen Doebert
- ...



## Motivation

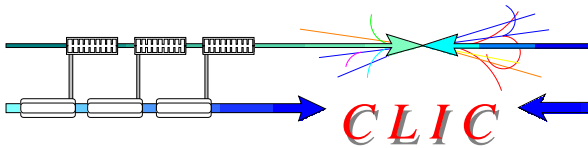


To provide rf designers with a local field quantity which limits high-power/high-gradient performance in the presence of rf breakdowns.

Make a theory and  
verify with  
measured data

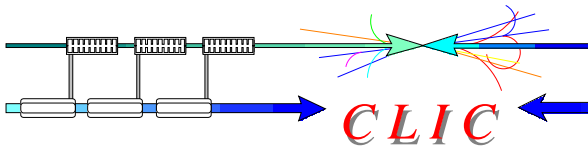
Make a fit to  
measured data  
and try to  
understand

# Introduction



The high-gradient performance depends on:

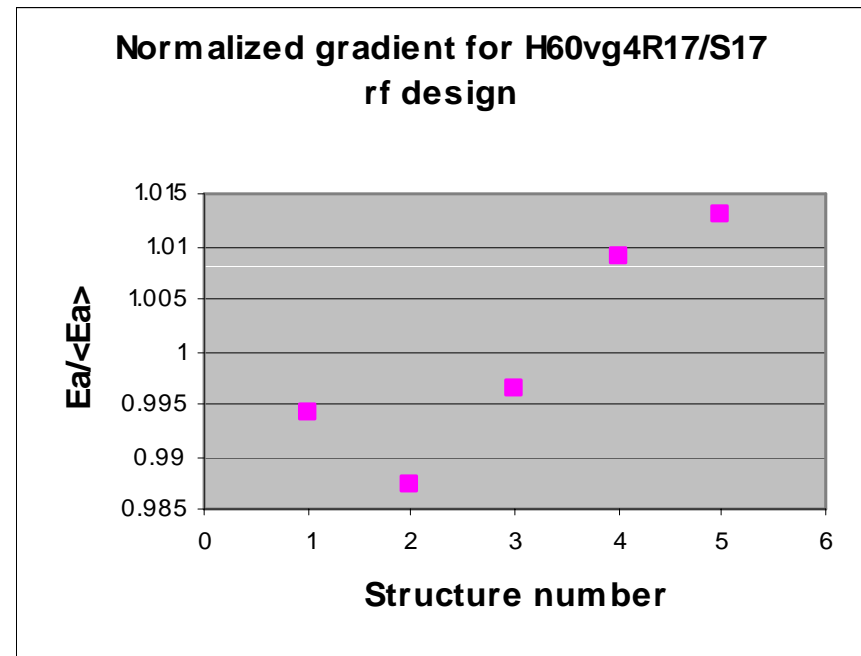
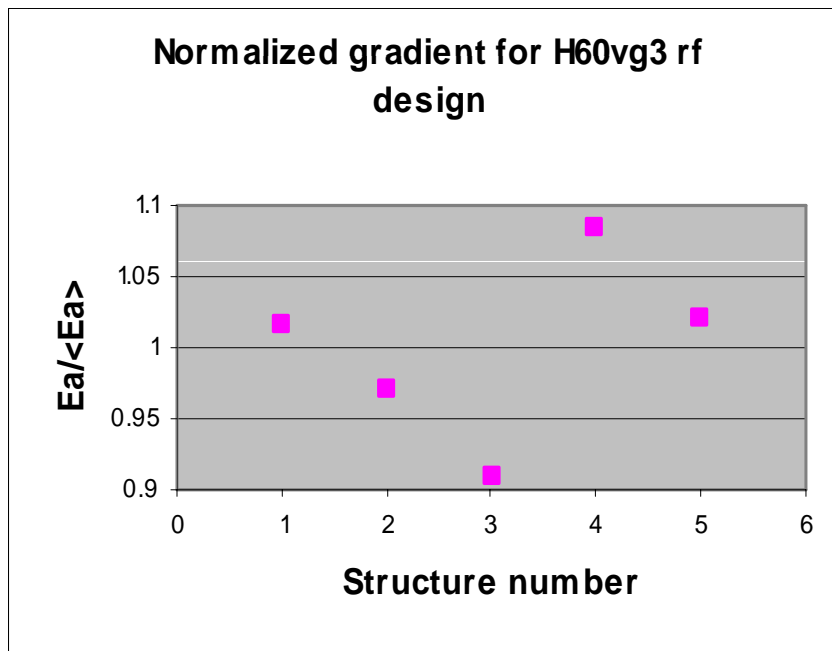
1. Geometry of the cavity: rf design
2. Surface of the cavity : anything else than rf design
  - Material
  - Heat treatment
  - Machining
  - Chemical treatment
3. Measurement technique and experimental setup



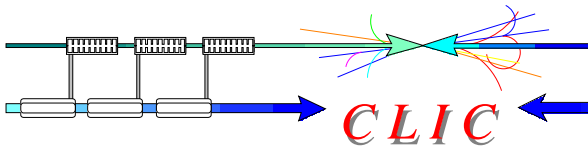
# Introduction



Variation of high-gradient performance of the same rf design.



N.B. Variation of up to tens of percents can be expected from the difference in the surface state, statistics and measurement setup.

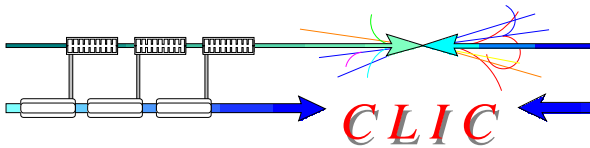


## Experimental data @ $BDR=10^{-6}$ , 100ns



	RF design name	f [GHz]	dphi [deg]	a1 [mm]	d1 [mm]	e1	vg1 [%]	Ea [MV/m]
1	DDS1	11.424	120	5.7	1	1	11.7	59.4
2	T53VG5R	11.424	120	4.45	1.66	1	5	80.9
3	T53VG3MC	11.424	120	3.9	1.66	1	3.3	102.2
4	H90VG3	11.424	150	5.3	4.2	1	3	77.7
5	H60VG3-FXB6	11.424	150	5.3	4.4	1	2.8	80.8
6	H60VG3S18	11.424	150	5.5	4.6	1.15	3.3	76.0
7	H60VG3S17-FXC5	11.424	150	5.3	3.7	1.34	3.6	83.3
8	H75VG4S18	11.424	150	5.3	3.04	1.36	4	101.0
9	H60VG4R17-2	11.424	150	5.68	3.65	1.37	4.5	82.6
10	HDX11-Cu	11.424	60	4.21	1.45	2.4	5.1	55.3
11	CLIC-X-band	11.424	120	3	2	1	1.1	120.4
12	SW20a565_1Cell	11.424	180	5.65	4.6	3.4	0	100.1
13	SW20a375	11.424	180	3.75	2.6	1.7	0	75.2
14	2pi/3	29.985	120	1.75	0.85	1	4.7	68.6
15	pi/2	29.985	90	2	0.85	1	7.4	48.7
16	HDS60L	29.985	60	1.9	0.55	2.5	8	45.5
17	HDS60S	29.985	60	1.6	0.55	2.4	5.1	55.8
18	HDS4Th	29.985	150	1.75	0.55	1	2.6	67.4
19	PETS9mm	29.985	120	4.5	0.85	1	39.8	16.4

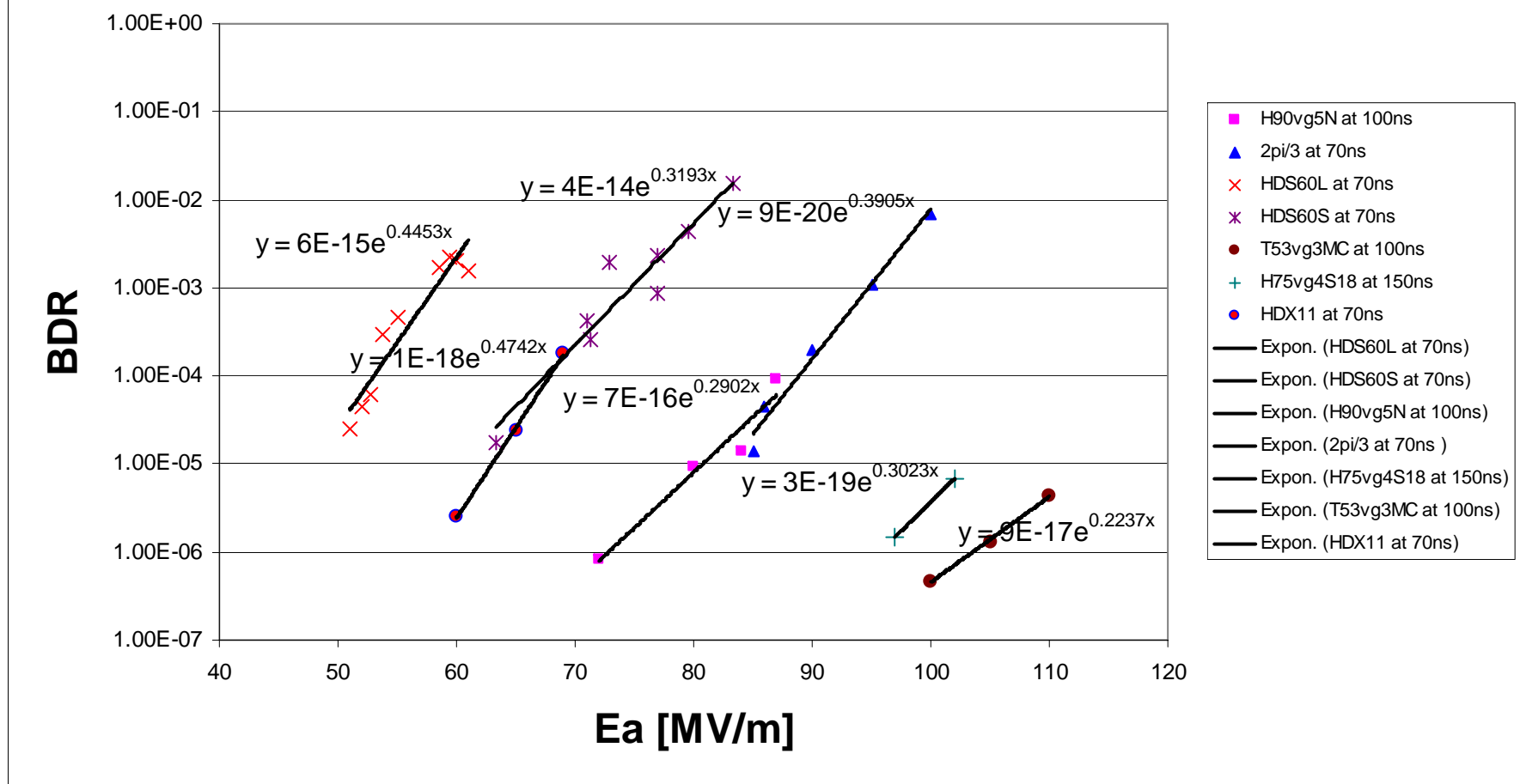
Measurement data were scaled to 100 ns pulse length and to  $BDR = 10^{-6}$ .



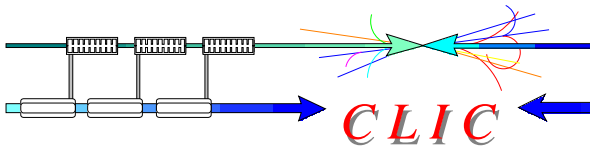
# BDR versus Gradient scaling



## BDR versus Gradient in Cu structures (expon. fit)



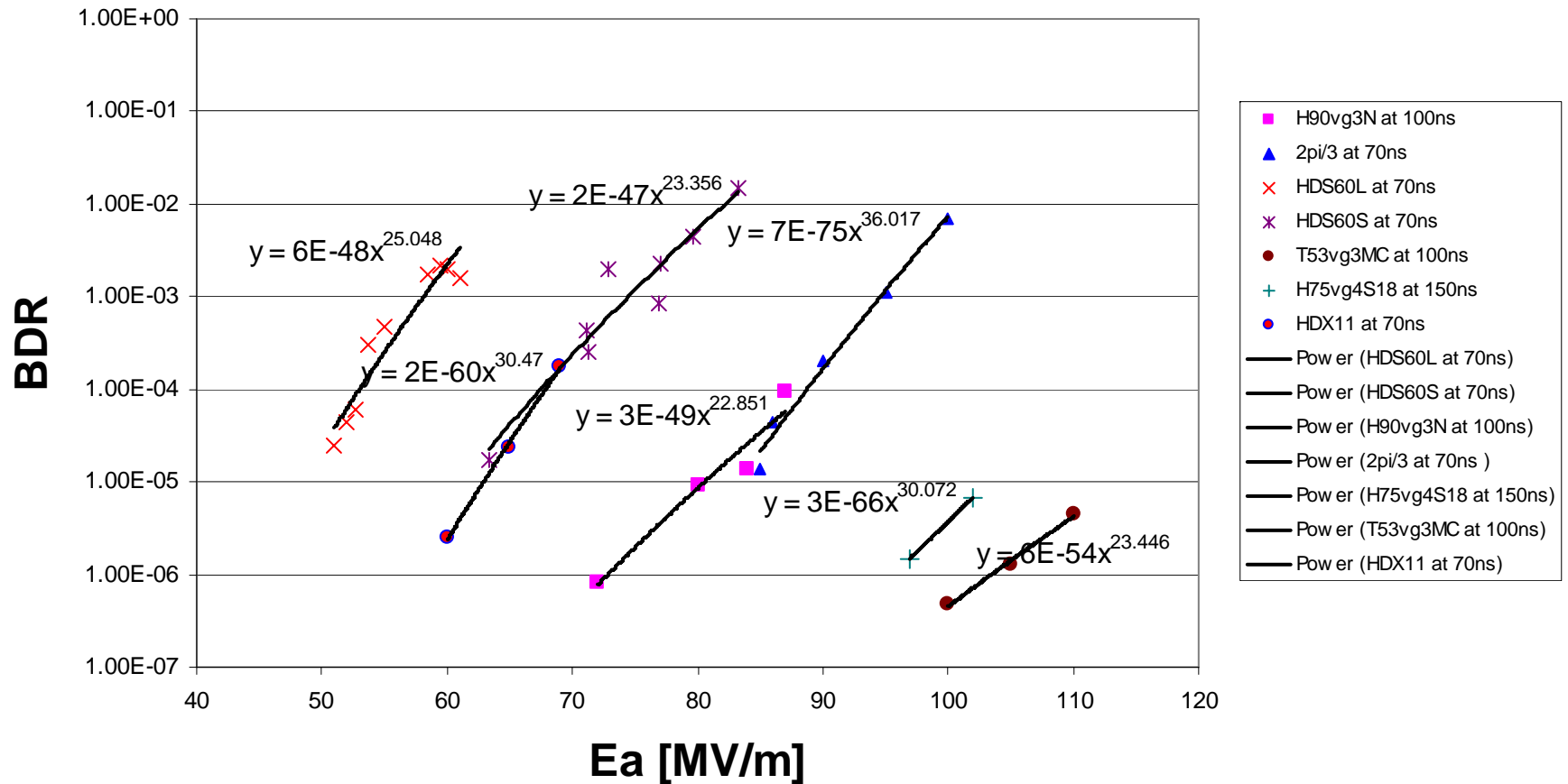
Exponential fit requires different slope depending on the gradient



# BDR versus Gradient scaling

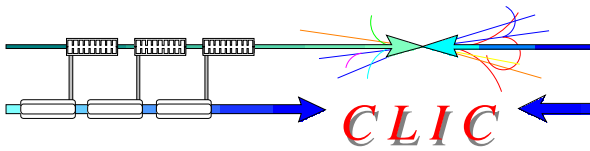


## BDR versus Gradient in Cu structures (power fit)

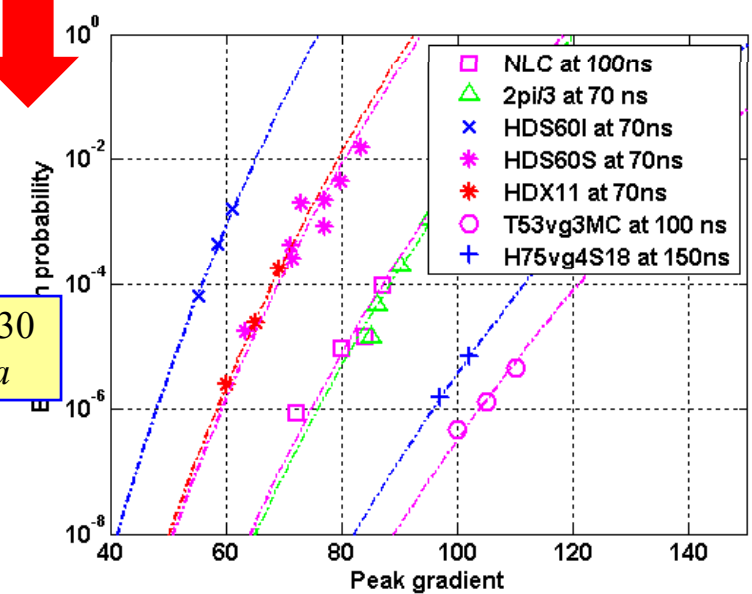
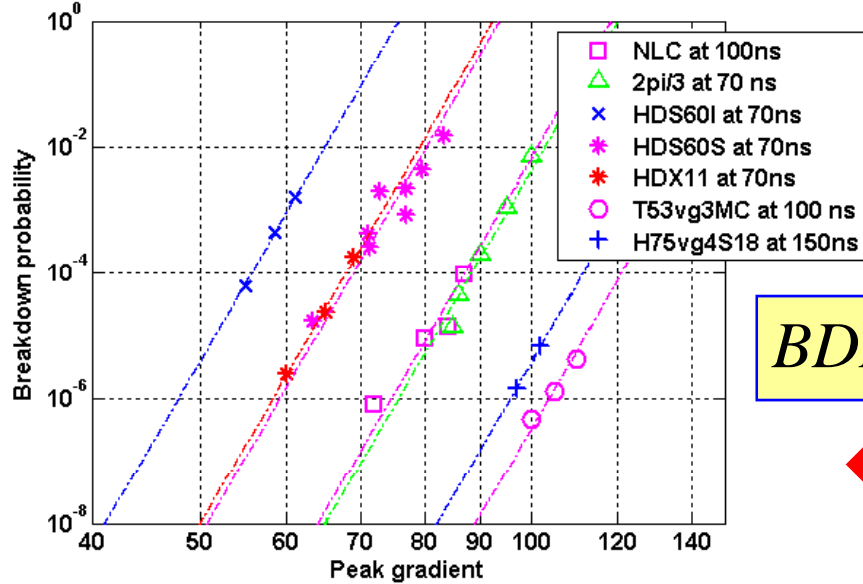
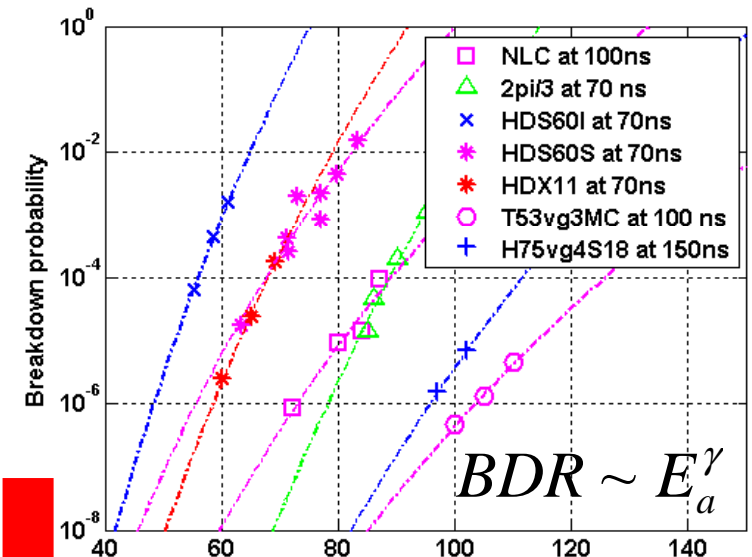
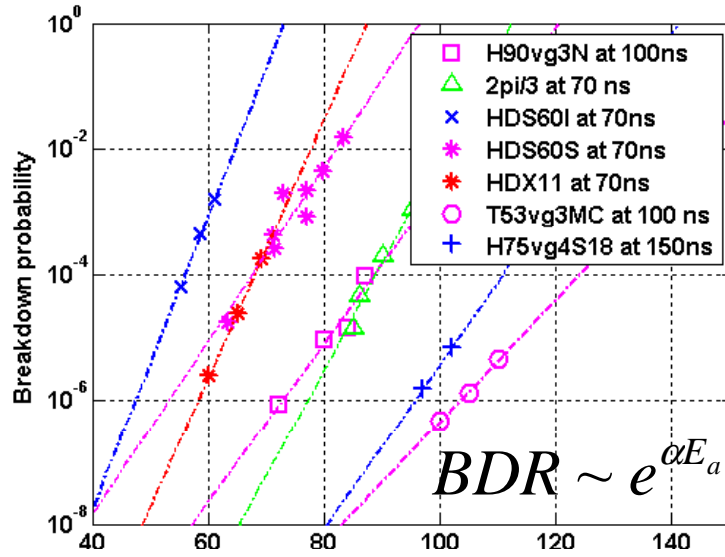


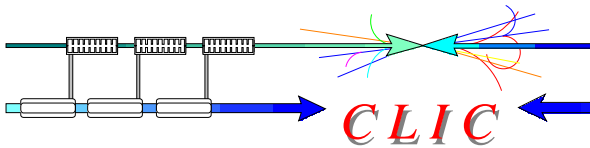
Power fit can be done with the same power for all gradients



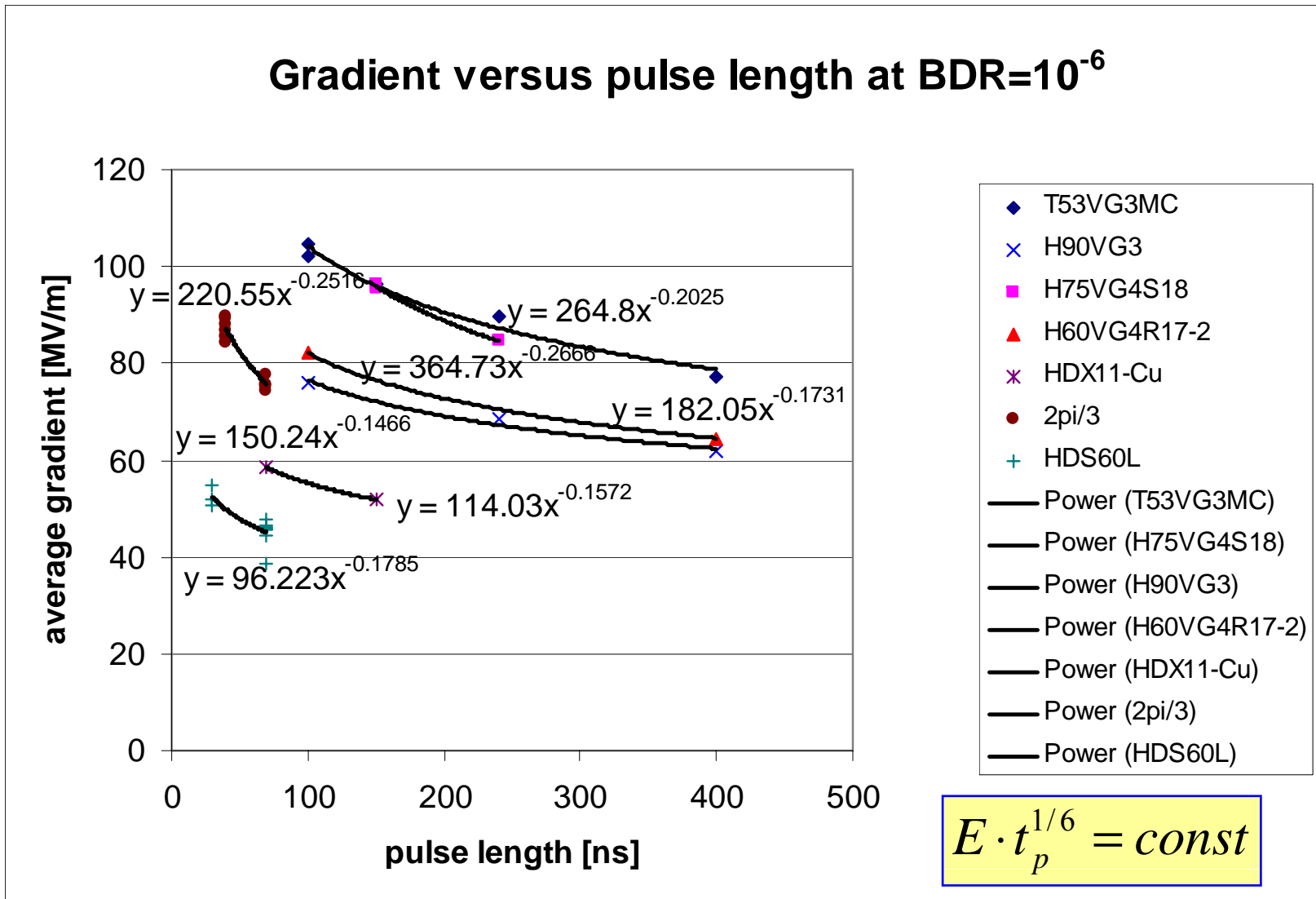


# BDR versus Gradient scaling

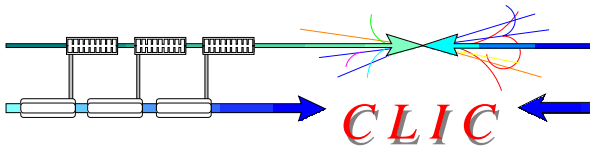




# Gradient versus pulse length scaling



N.B. This is very well known scaling law being confirmed again and again



## Summary on gradient scaling



For a fixed pulse length

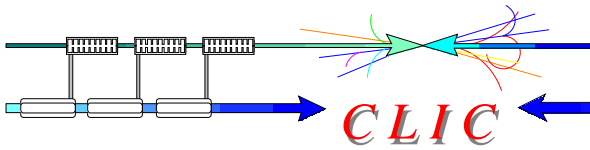
$$BDR \sim E_a^{30}$$

For a fixed BDR

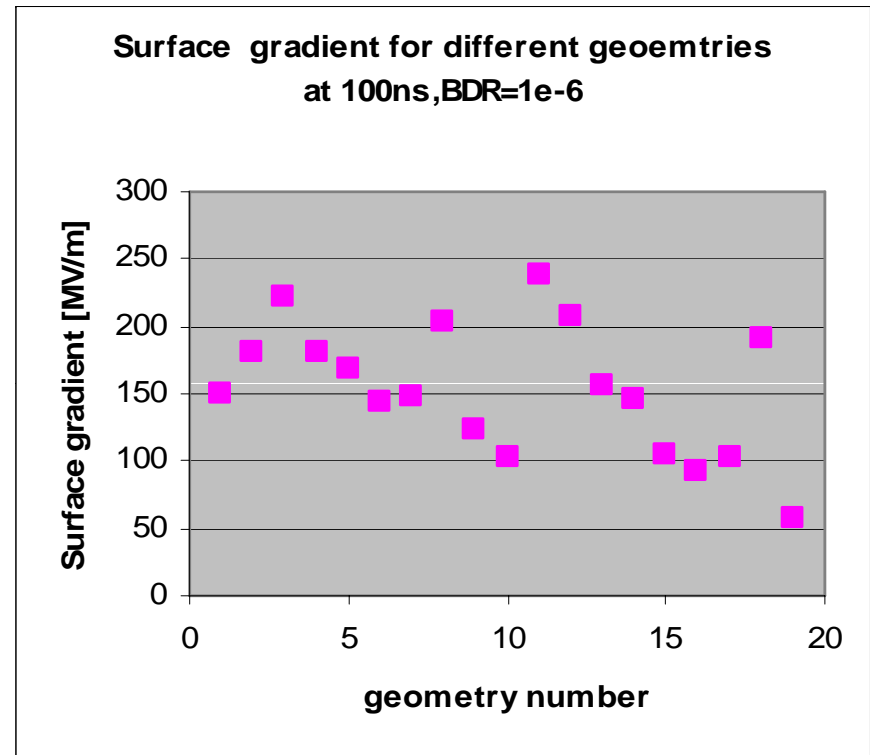
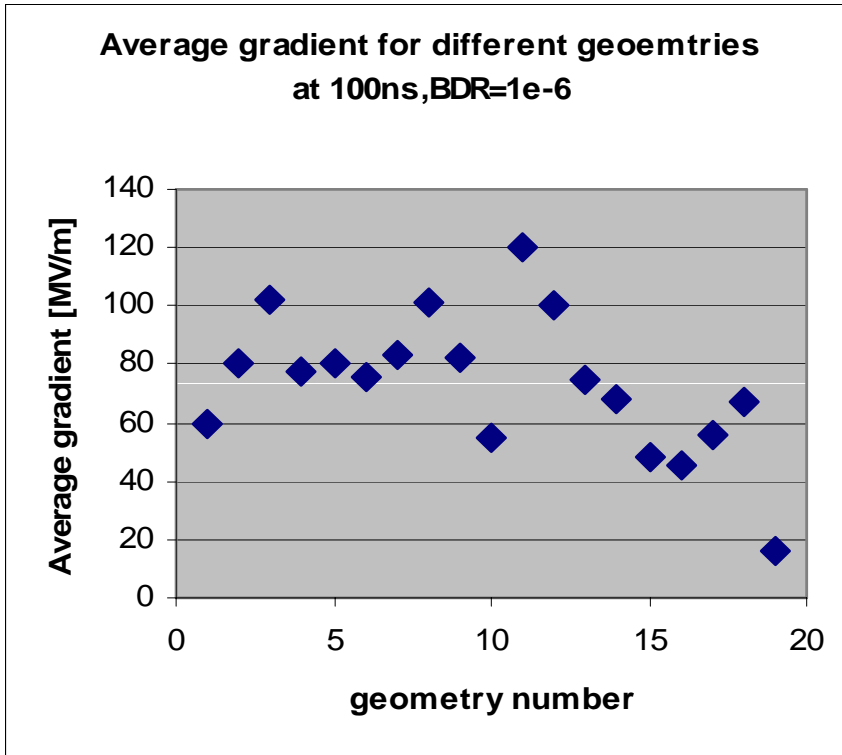
$$E_a \cdot t_p^{1/6} = const$$

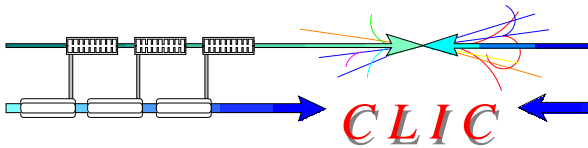
$$\frac{E_a^{30} \cdot t_p^5}{BDR} = const$$

- In a Cu structure, ultimate gradient  $E_a$  can be scaled to certain BDR and pulse length using above power law. It has been used in the following analysis of the data.
- The aim of this analysis is to find a field quantity  $X$  which is geometry independent and can be scaled among all Cu structures.

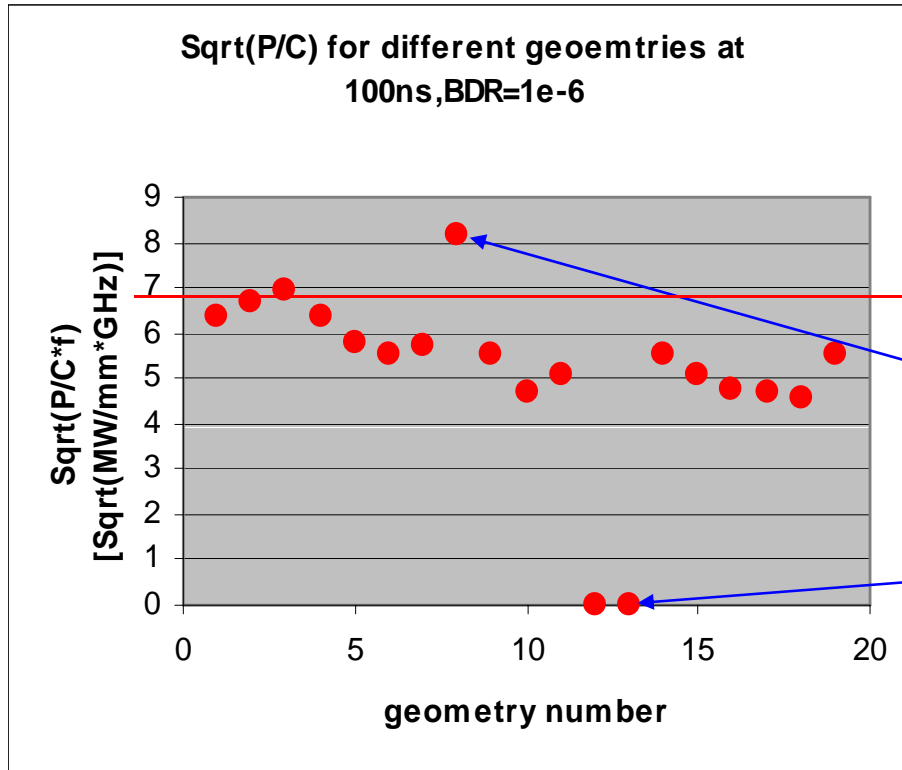


# Accelerating and surface gradients





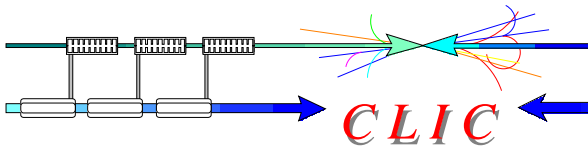
# Power over circumference



Much better agreement  
but

18Wu

1. This is not a local field quantity.
2. H75vg4S18 does not really fit.
3. Does not describe standing wave structures.

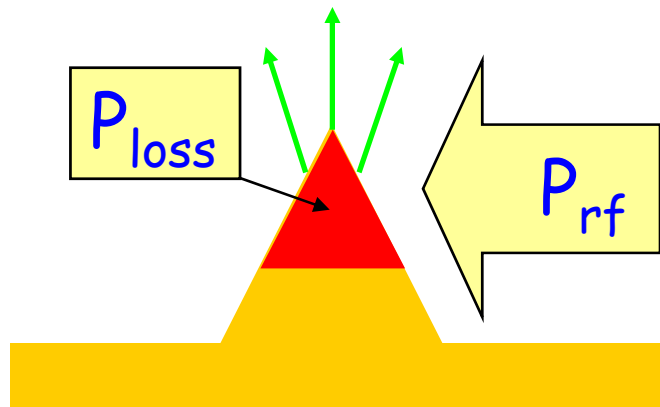


## Breakdown initiation scenario



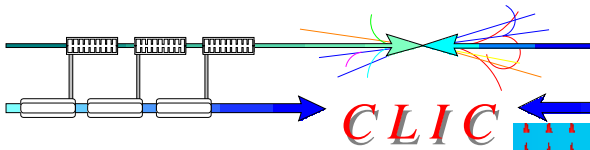
### Qualitative picture

- Field emission currents  $J_{FN}$  heat a (potential) breakdown site up to a temperature rise  $\Delta T$  on each pulse.
- After a number of pulses the site got modified so that  $J_{FN}$  increases so that  $\Delta T$  increases above a certain threshold.
- Breakdown takes place.

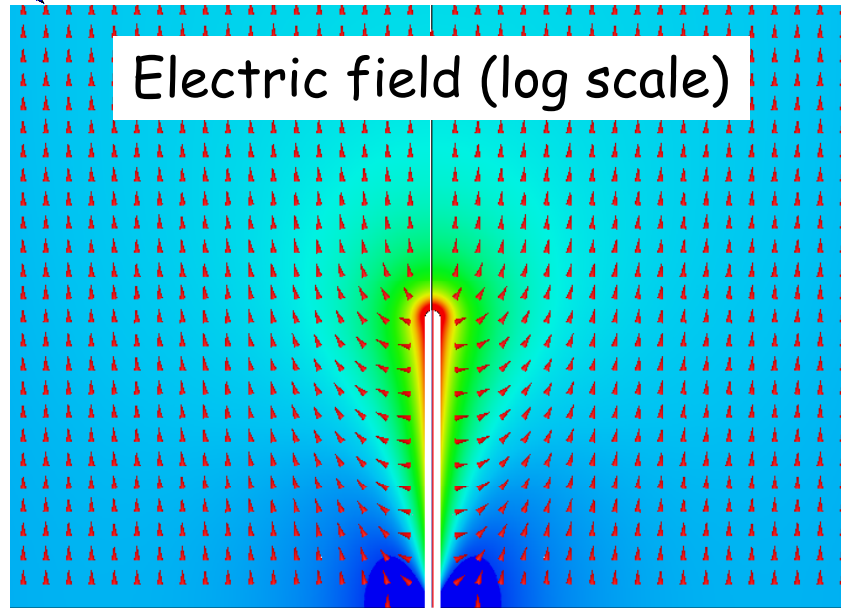


This scenario can explain:

- Dependence of the breakdown rate on the gradient (Fatigue)
- Pulse length dependence of the gradient (1D÷3D heat flow from a point-like source)



# EM fields around a tip of $\beta=30$



Unperturbed  
rf power flow:

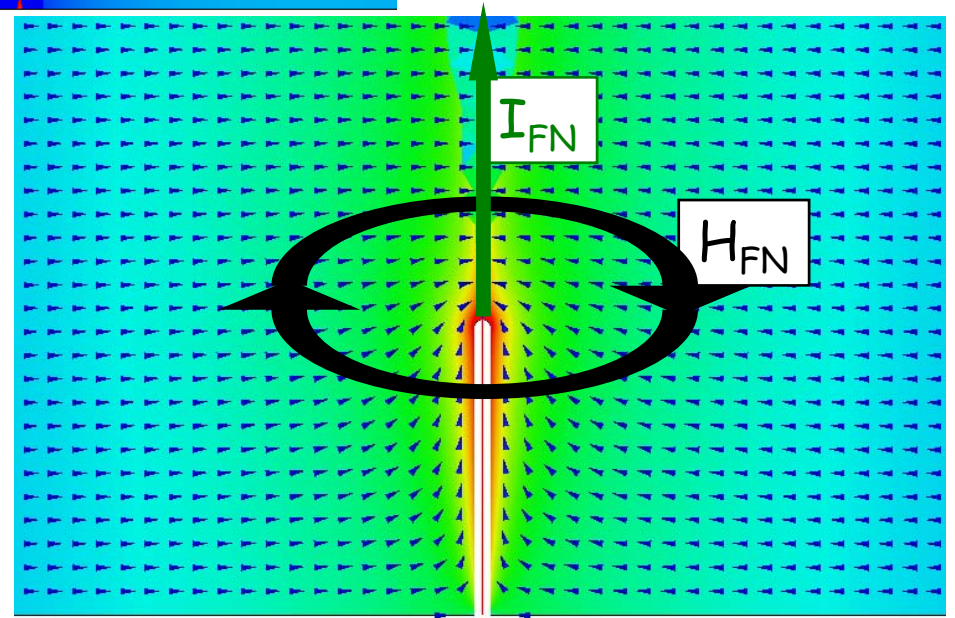
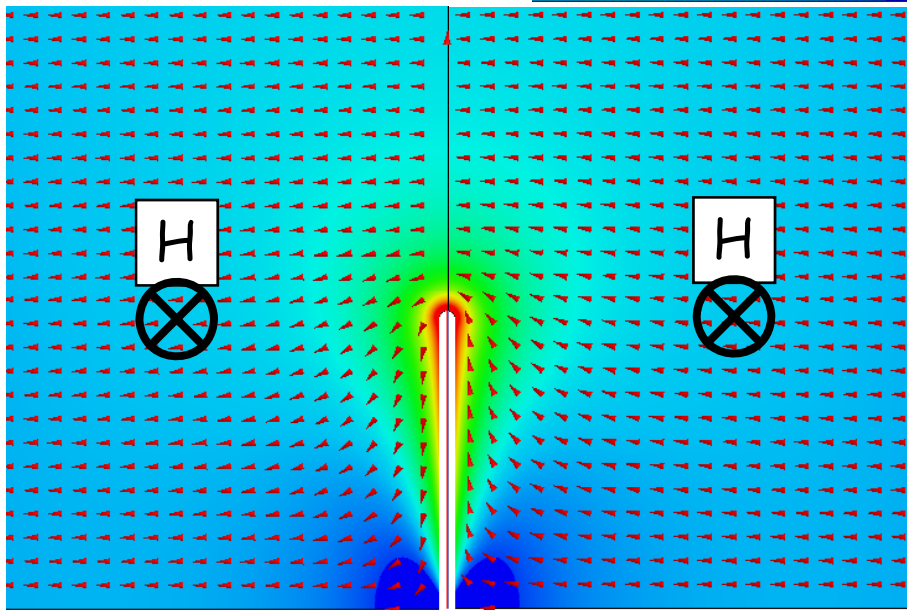
$$S = E \times H$$

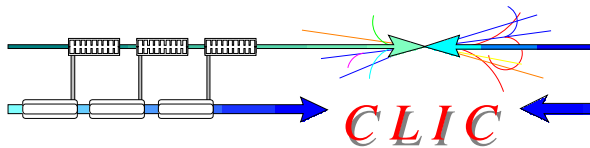
$$H = \text{const}$$

Field emission  
power flow:

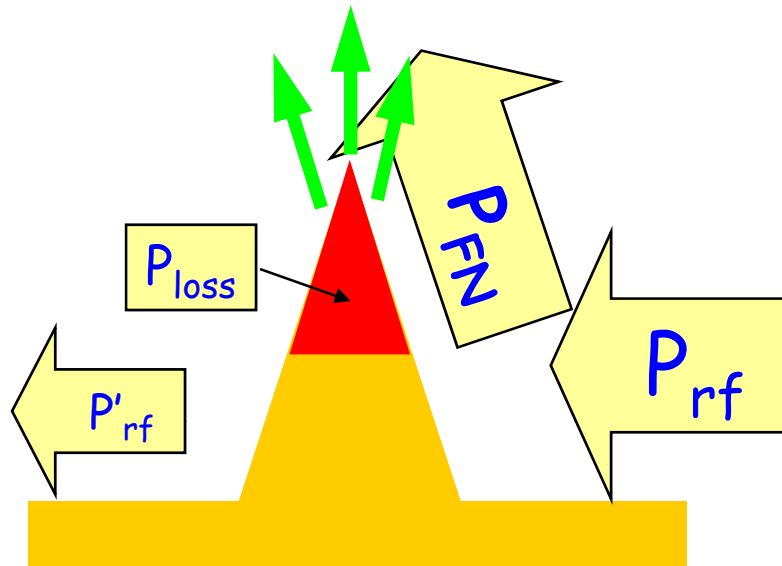
$$S_{\text{FN}} = E \times H_{\text{FN}}$$

$$H_{\text{FN}} = I_{\text{FN}} / 2\pi r$$





## Field emission and rf power flow



$$\Delta T \sim P_{loss} \ll P_{FN} \leq P_{rf}$$

$$P_{loss} = \int_V J_{FN}^2 \rho \, dv$$

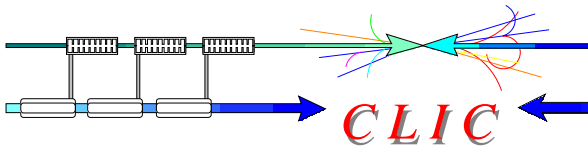
$$P_{FN} = \oint_S \mathbf{E} \times \mathbf{H}_{FN} \, ds \sim \mathbf{E} \cdot \mathbf{I}_{FN}$$

$$P_{rf} = \oint_S \mathbf{E} \times \mathbf{H} \, ds$$

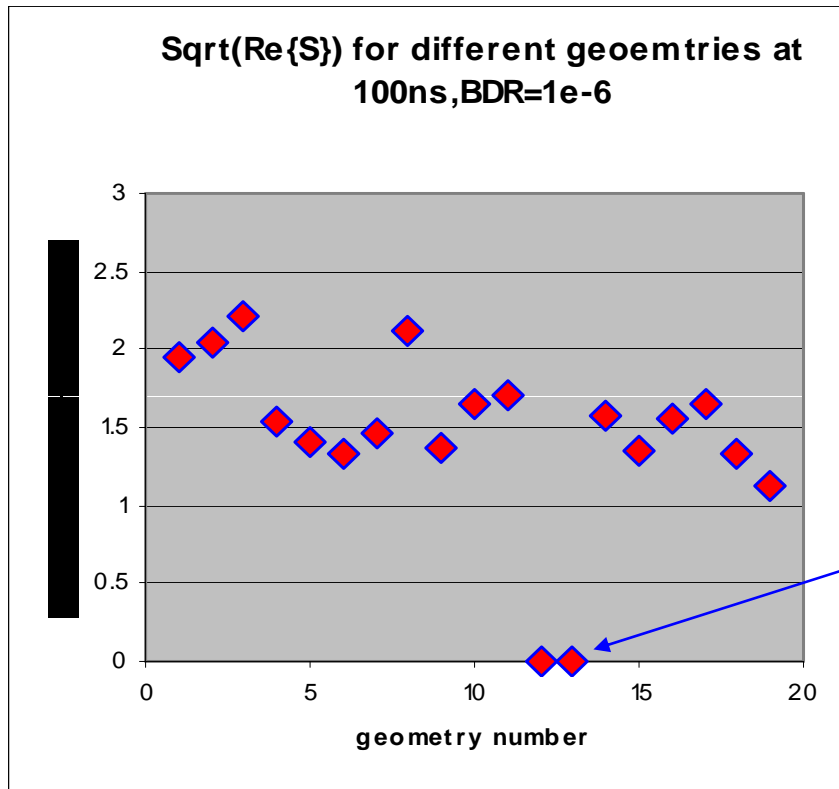
There are two regimes depending on the level of rf power flow

1. If the rf power flow dominates, the electric field remains unperturbed by the field emission currents and heating is limited by the rf power flow (We are in this regime)
2. If power flow associated with field emission current  $P_{FN}$  dominates, the electric field is reduced due to "beam loading" thus limiting field emission and heating



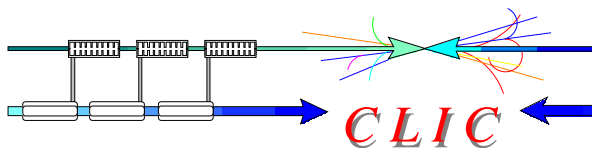


# Active power flow density



Real part of Poynting vector:  
 $P_{rf} \sim \text{Re}\{S\} = \text{Re}\{E \times H\}$

1. This is a local field quantity.
2. H75vg4S18 fits.
3. Still does not describe standing wave structures.

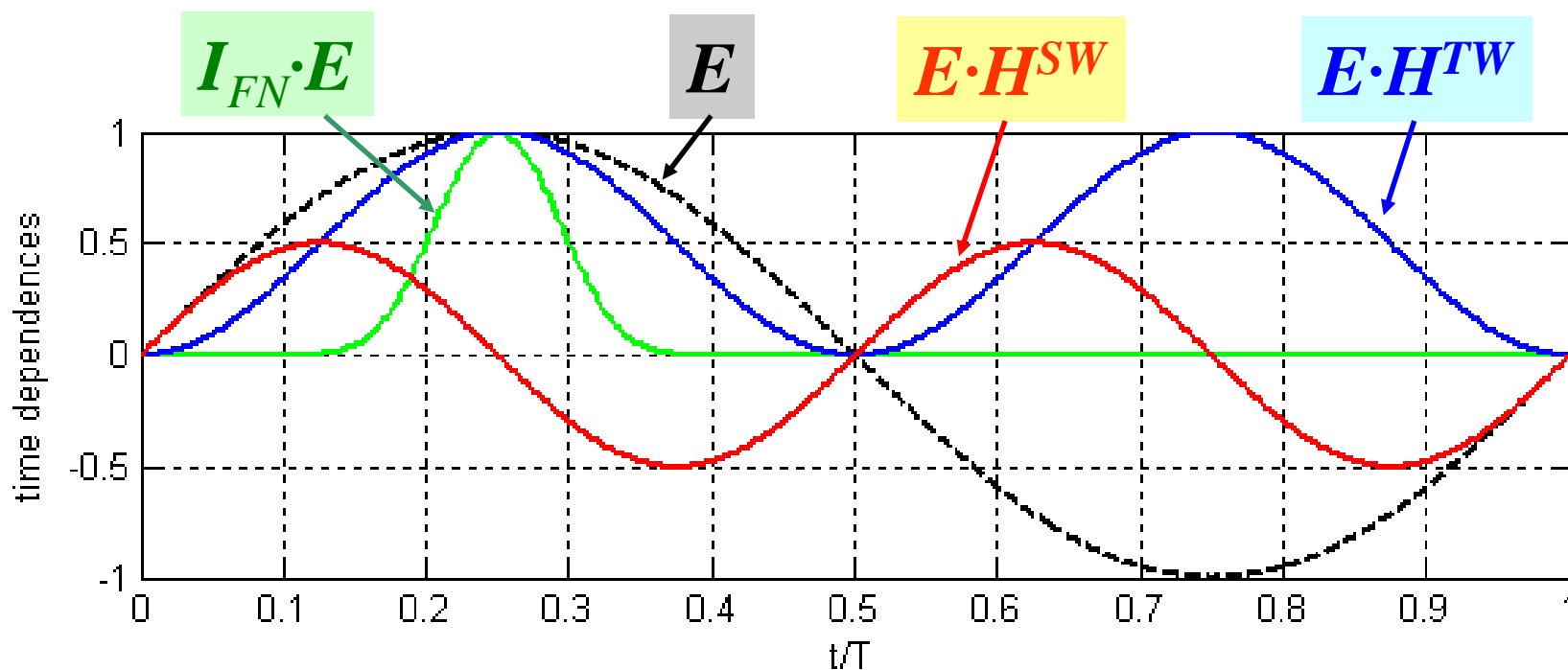


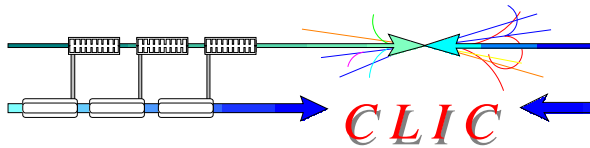
## Field emission and power flow



$$E \times H = E_0 \cdot H_0^{TW} \sin^2 \omega t + E_0 \cdot H_0^{SW} \sin \omega t \cos \omega t$$

$$I_{FN} \cdot E = A E_0^3 \sin^3 \omega t \cdot \exp\left(\frac{-62 \text{ GV/m}}{\beta E_0 \sin \omega t}\right)$$





## Field emission and rf power coupling



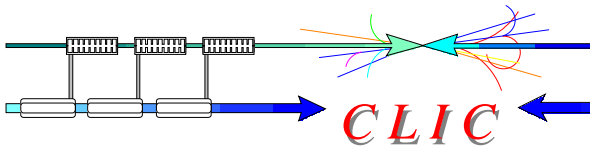
What matters for the breakdown is the amount of rf power **coupled** to the field emission power flow.

$$P_{coup} = \int_0^{T/4} P_{rf} \cdot P_{FN} dt \bigg/ \left( \int_0^{T/4} P_{FN} dt \cdot \int_0^{T/4} P_{rf} dt \right)$$

$$= C^{TW} E_0 H_0^{TW} + C^{SW} E_0 H_0^{SW}$$

Assuming that all breakdown sites have the same geometrical parameters the breakdown limit can be expressed in terms of modified Poynting vector  $S_c$ .

$$S_c = E_0 H_0^{TW} + \frac{C^{SW}}{C^{TW}} E_0 H_0^{SW} = \text{Re}\{\mathbf{S}\} + g_c \cdot \text{Im}\{\mathbf{S}\}$$

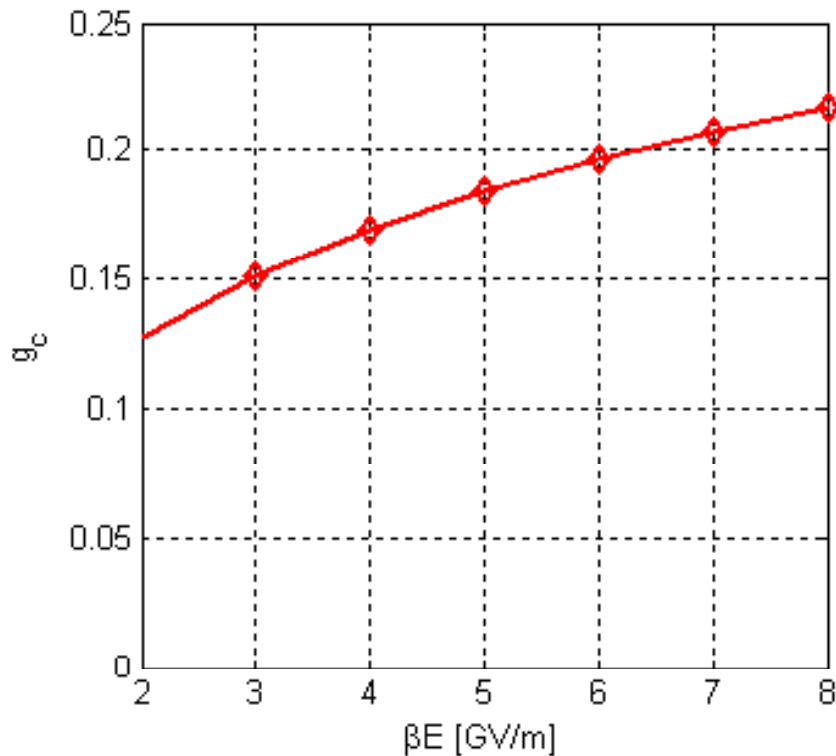


## Field emission and rf power coupling

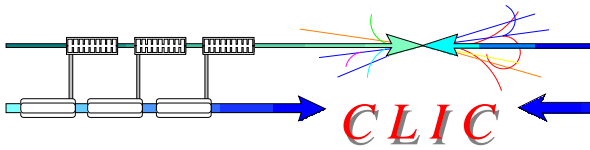


Constant  $g_c$  depends only on the value of the local surface electric field  $\beta E_0$

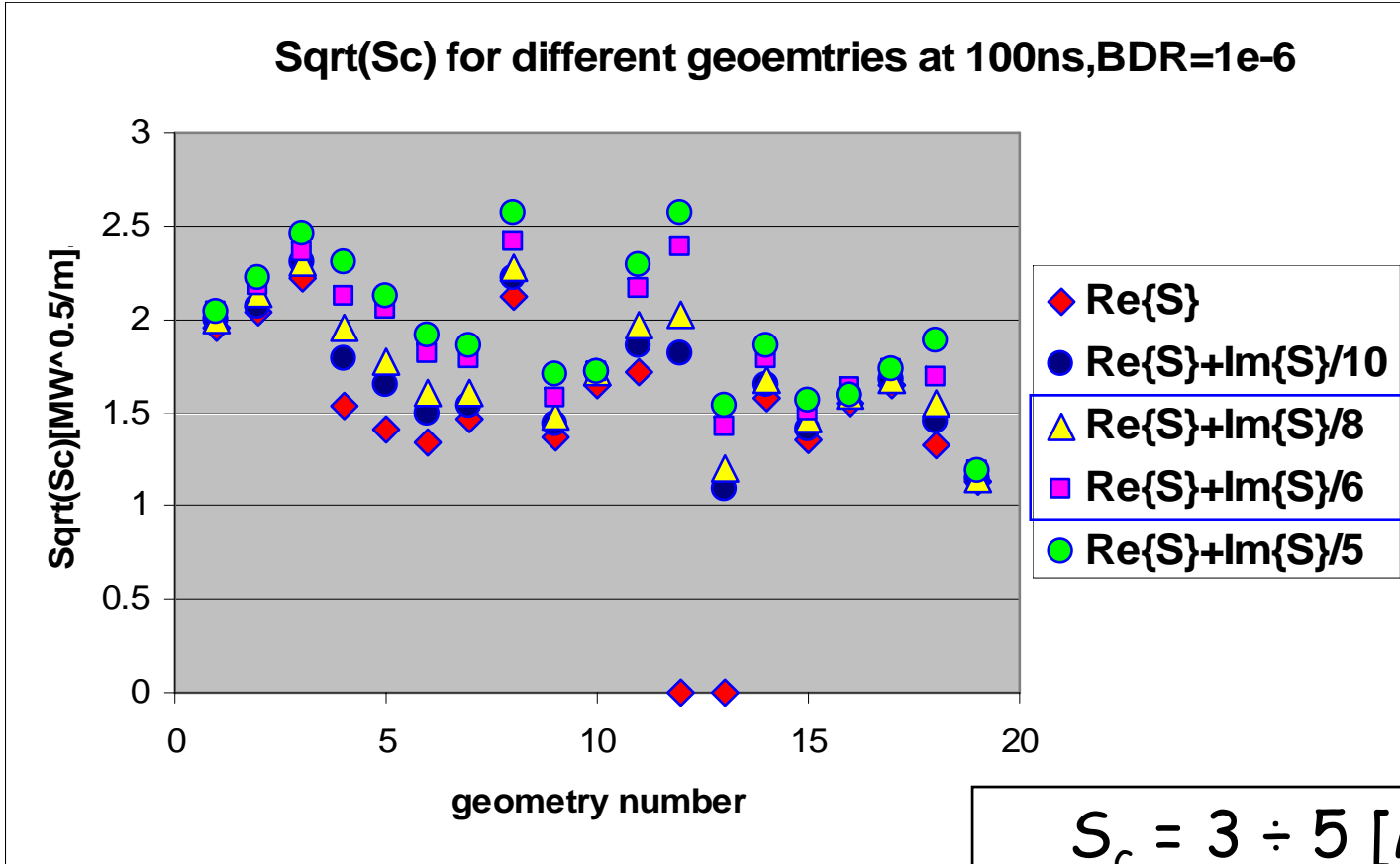
$$g_c = \frac{\int_0^{\pi/2} \sin^4 x \cos x \cdot \exp\left(\frac{-62 \text{ GV/m}}{\beta E_0 \sin x}\right) dx}{\int_0^{\pi/2} \sin^5 x \cdot \exp\left(\frac{-62 \text{ GV/m}}{\beta E_0 \sin x}\right) dx}$$



$g_c$  is in the range:  
from 0.15 to 0.2



# New rf breakdown constraint $S_c$



- ◆ Re{S}
- Re{S}+Im{S}/10
- ▲ Re{S}+Im{S}/8
- Re{S}+Im{S}/6
- Re{S}+Im{S}/5

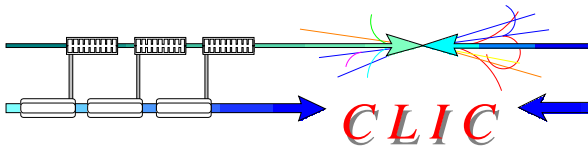
Look good

$$S_c = \text{Re}\{S\} + \text{Im}\{S\} / (6 \div 8)$$

$$S_c = 3 \div 5 \text{ [MW/mm}^2\text{]}$$

at 100ns, BDR=1e-6

$$S_c^{15} t_p^5 / \text{BDR} = \text{const}$$



$$S_{c6} = \text{Re}\{S\} + \text{Im}\{S\}/6 \text{ in CLIC}_G$$

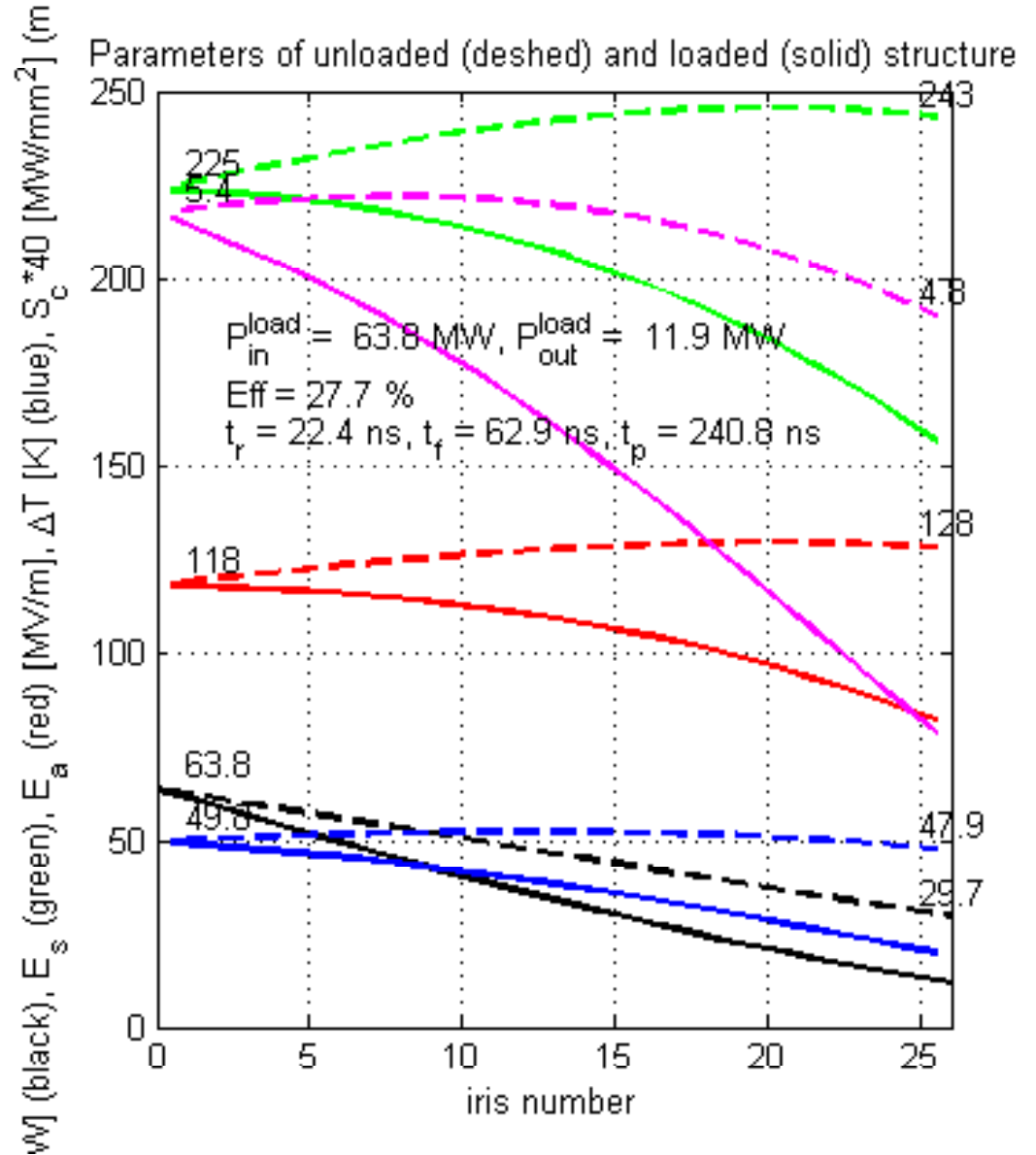
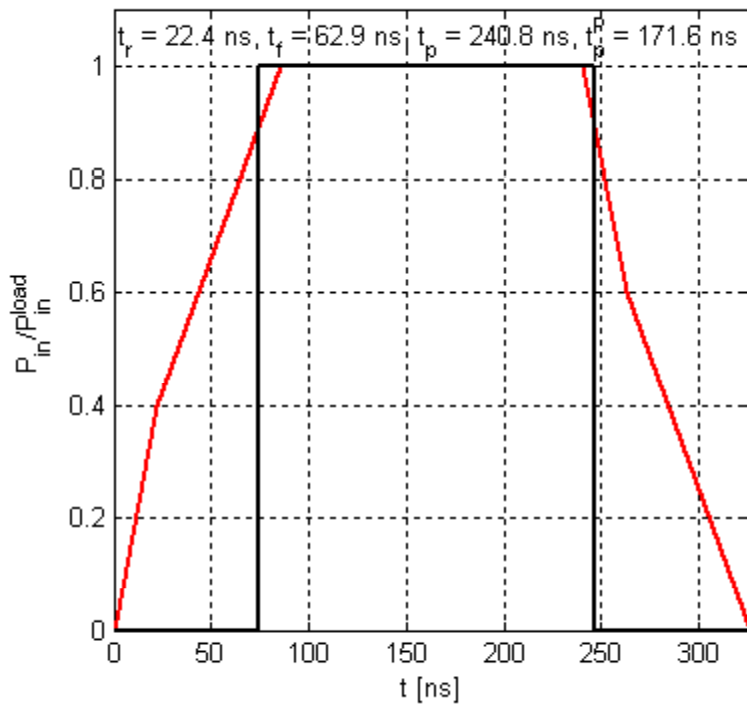


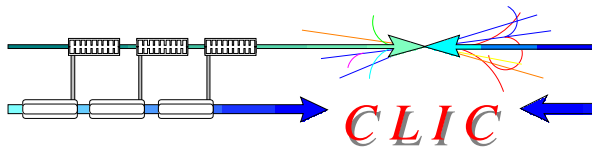
$S_{c6}$  reaches 5.55 for nominal parameters.

Scaling it to 100ns gives:

$$5.55 \cdot (171.6/100)^{1/3} = 6.64$$

To be compared with the measured data.

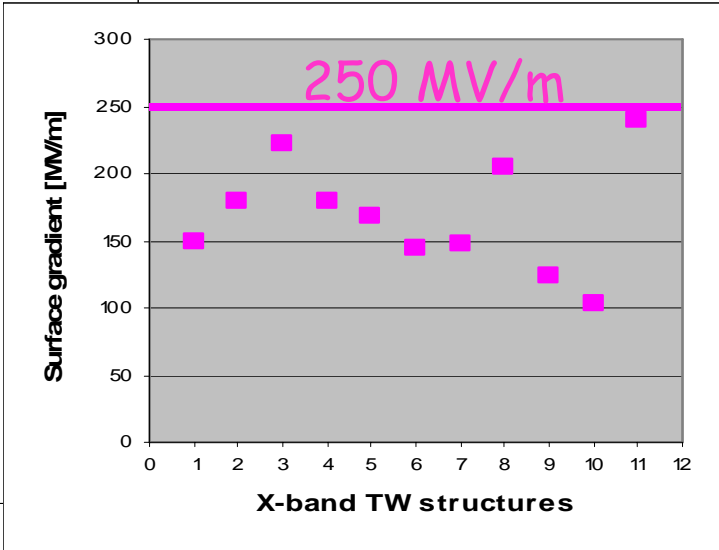
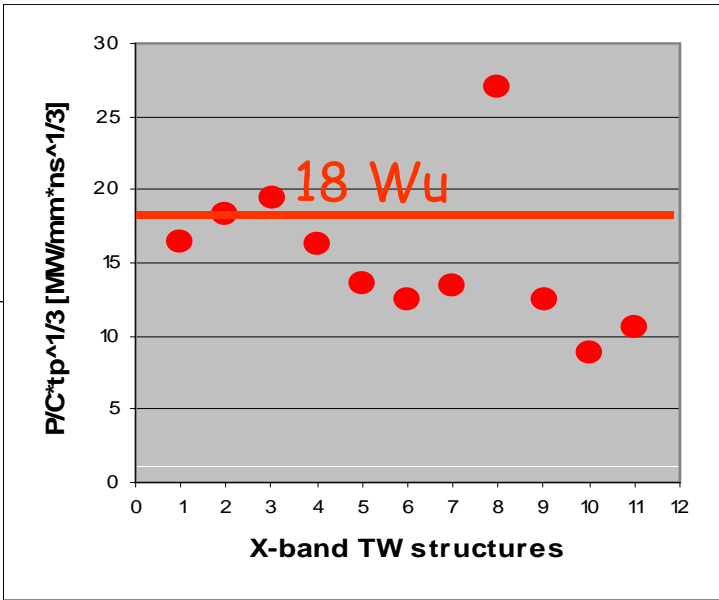
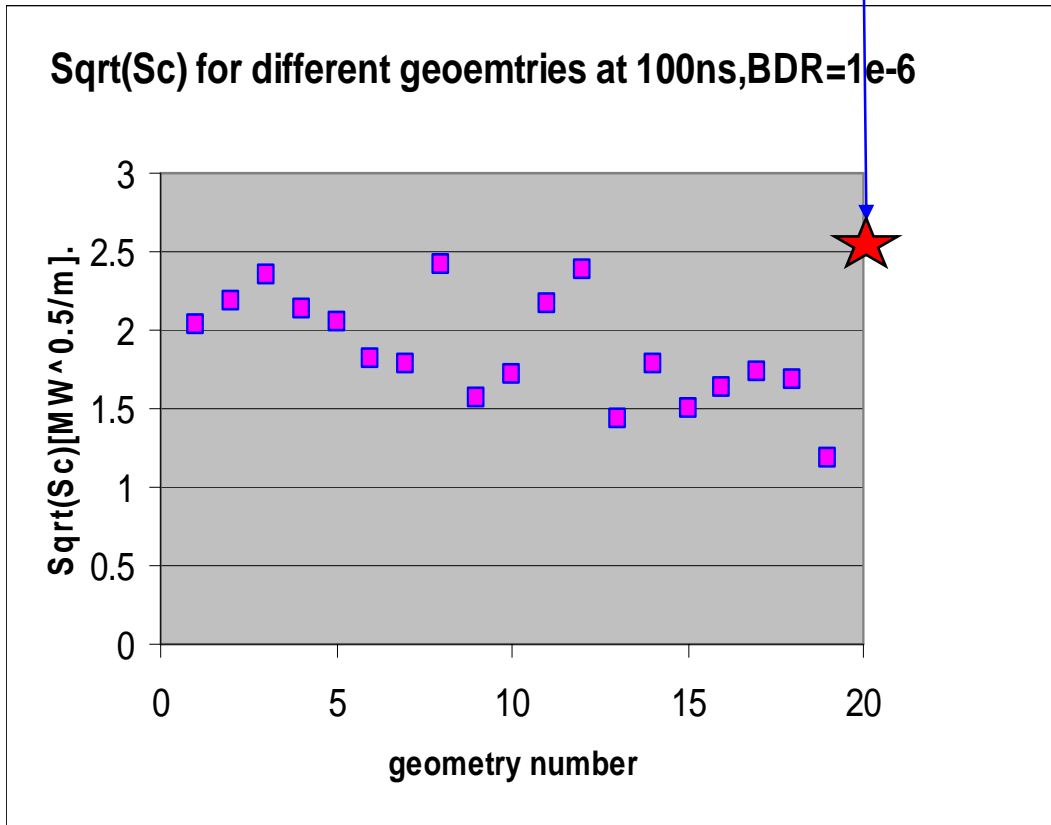


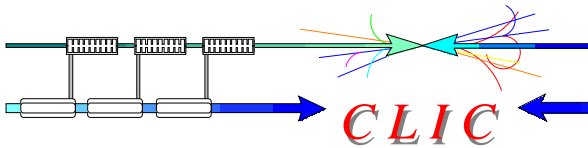


# $S_{c6}$ in CLIC\_G



$S_{c6}$  values in CLIC\_G for the nominal parameters is very challenging



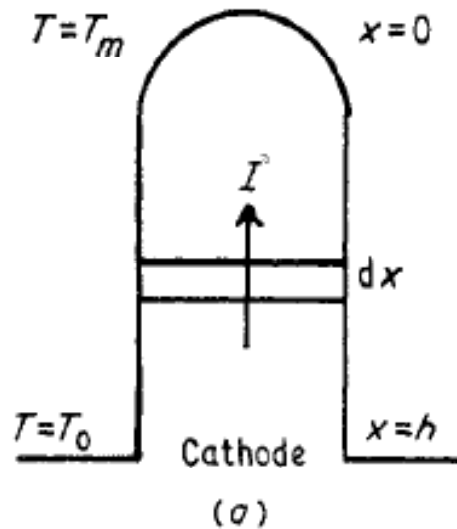


## Analytical estimates for a cylindrical tip



For a cylindrical protrusion heat conduction is described by:

$$C_v \frac{\partial T}{\partial t} = K \frac{\partial^2 T}{\partial x^2} + J^2 \rho$$

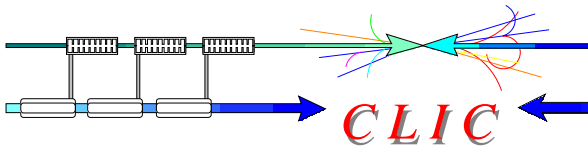


Let's get approximate solution it in two steps:

1. Solve it in steady-state (i.e. left hand side is zero) for a threshold current density required to reach melting temperature  $T_m$
2. Solve time dependent equation in linear approximation to get the threshold time required to reach melting temperature

Williams & Williams,  
J. Appl. Phys. D,  
5 (1972) 280





## Analytical estimates for a cylindrical tip



Case A: Resistivity is temperature independent:

$$\rho = \rho_0$$

Step 1:

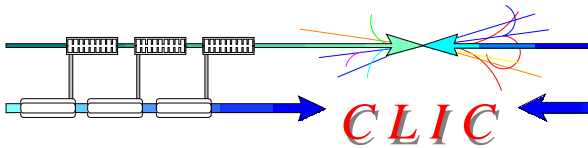
$$K \frac{\partial^2 T}{\partial x^2} + J^2 \rho_0 = 0; \quad T|_{x=h} = T_0; \quad T|_{x=0} = T_m; \quad \left. \frac{\partial T}{\partial x} \right|_{x=0} = 0$$

$$T = T_m - \frac{J^2 \rho_0}{2K} x^2; \quad J_m^{\rho_0} = \sqrt{\frac{2K(T_m - T_0)}{h^2 \rho_0}}$$

Step 2:

$$C_V \frac{\partial T}{\partial t} = J^2 \rho; \quad T|_{t=0} = T_0; \quad T|_{t=t_m} = T_m$$

$$T = T_0 + \frac{J^2 \rho_0}{C_V} t; \quad \tau_m^{\rho_0} = \frac{C_V (T_m - T_0)}{J_m^{\rho_0} \rho_0} = \frac{C_V}{K} \frac{h^2}{2}$$



## Analytical estimates for a cylindrical tip



Case B: Resistivity is temperature-dependent:  $\rho = \rho_0 \cdot T/T_0$  (Bloch-Grüneisen)

Step 1:

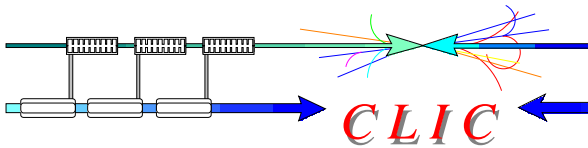
$$K \frac{\partial^2 T}{\partial x^2} + J^2 \rho = 0; \quad T|_{x=h} = T_0; \quad T|_{x=0} = T_m; \quad \left. \frac{\partial T}{\partial x} \right|_{x=0} = 0$$

$$T = T_m \cos \sqrt{\frac{J^2 \rho_0}{KT_0}} x; \quad J_m^{\rho 1} = \sqrt{\frac{KT_0}{h^2 \rho_0}} \arccos \frac{T_0}{T_m}$$

Step 2:

$$C_V \frac{\partial T}{\partial t} = J^2 \rho; \quad T|_{t=0} = T_0; \quad T|_{t=t_m} = T_m$$

$$T = T_0 \exp \frac{J^2 \rho_0}{C_V T_0} t; \quad \tau_m^{\rho 1} = \frac{C_V T_0}{J^2 \rho_0} \ln \frac{T_m}{T_0} = \frac{C_V}{K} h^2 \ln \frac{T_m}{T_0} / \arccos^2 \frac{T_0}{T_m}$$

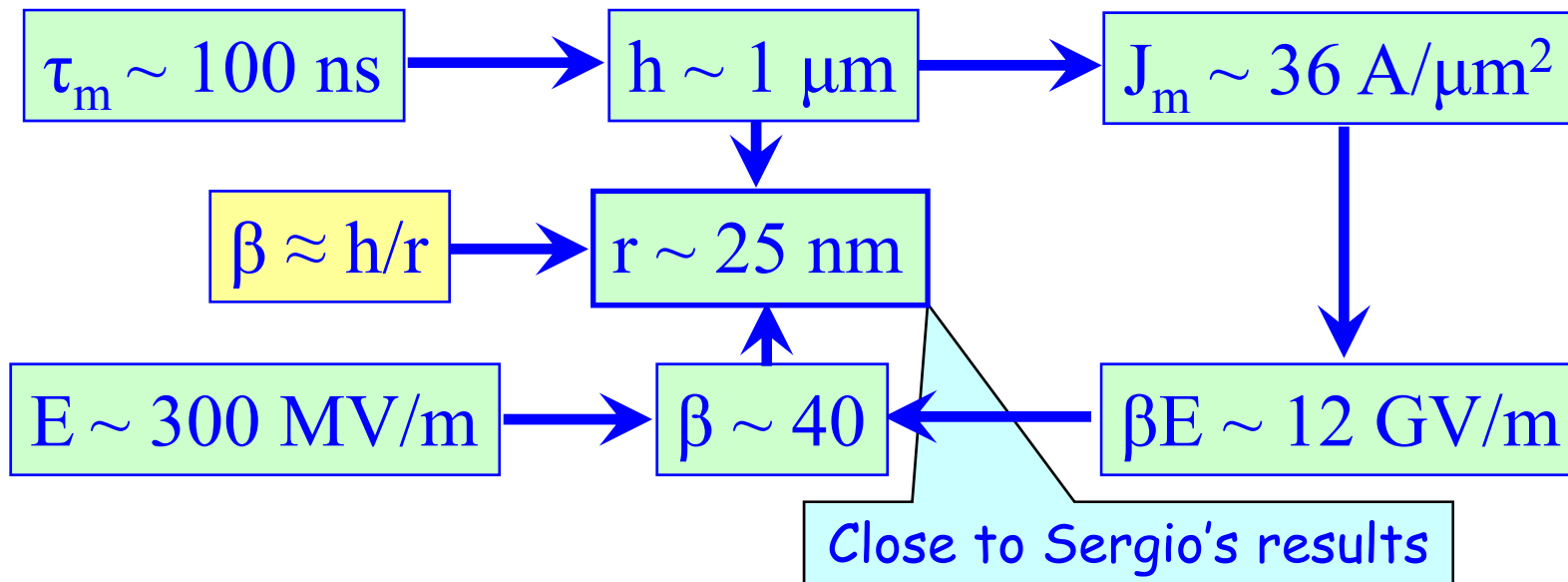


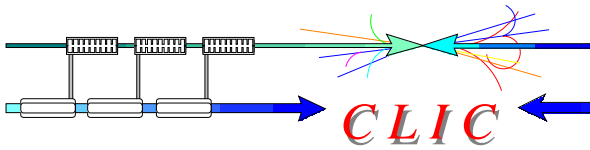
## Analytical estimates for a cylindrical tip



Fundamental constants for copper	
Thermal conductivity: $K$ [W/m·K]	400
Volumetric heat capacity: $C_V$ [MJ/m <sup>3</sup> ·K]	3.45
Resistivity@300K: $\rho_0$ [nΩ·m]	17
Melting temperature: $T_m$ [K]	1358

Some numbers for Case B:  $\rho = \rho_0 \cdot T/T_0$





# Analytical estimates for a cylindrical tip



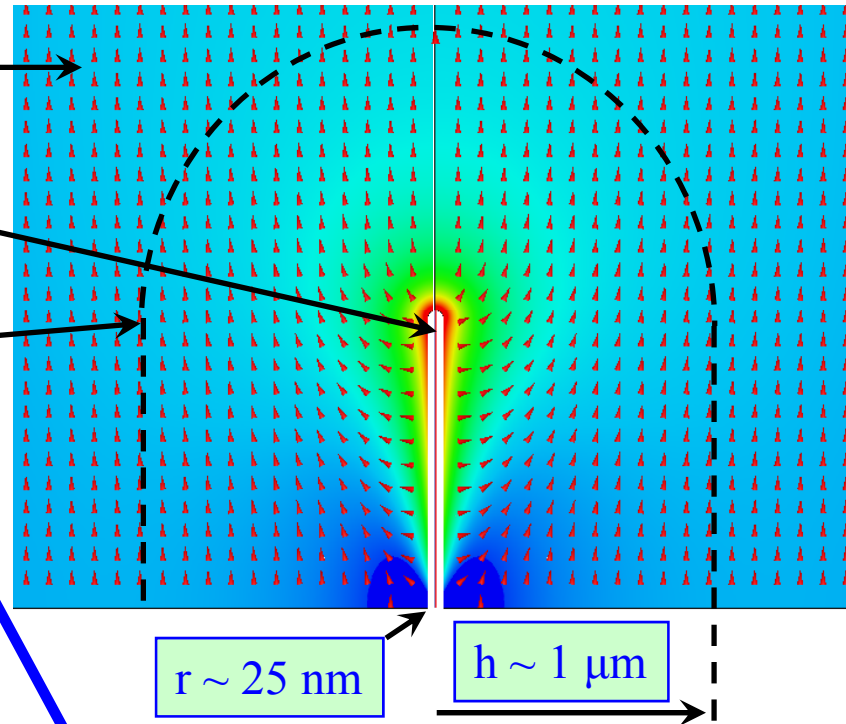
Some numbers for Case 2:  $\rho = \rho_0 \cdot T/T_0$  (Continue)

$\beta \sim 40$

$E \sim 300 \text{ MV/m}$

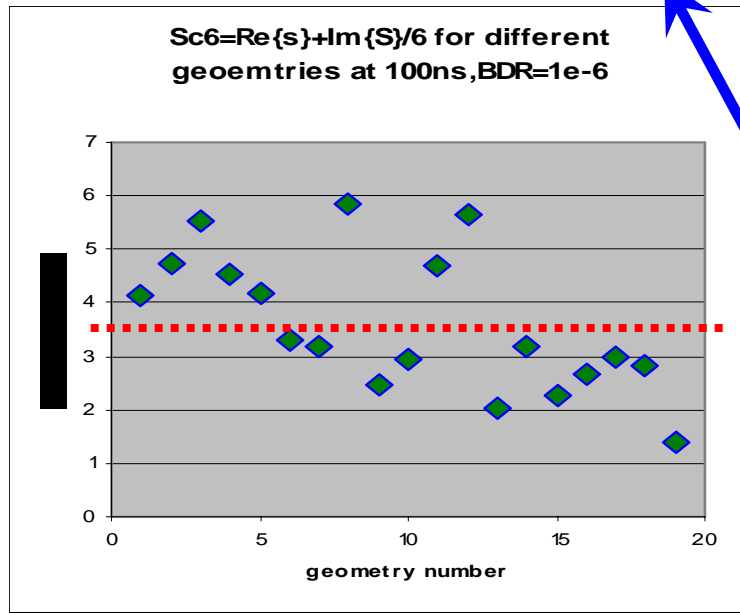
$J_m \sim 36 \text{ A}/\mu\text{m}^2$

$S_{FN} \sim 3.4 \text{ W}/\mu\text{m}^2$

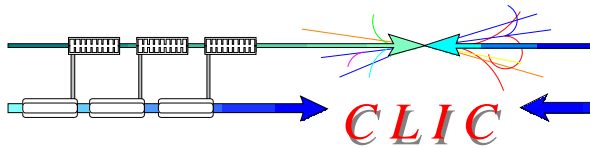


$r \sim 25 \text{ nm}$

$h \sim 1 \mu\text{m}$



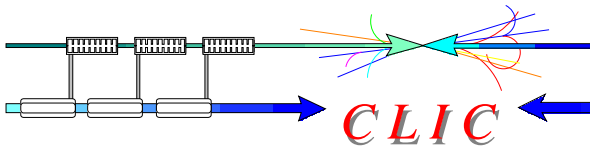
$$S_{FN}|_h = E H_{FN} = E \frac{J \pi r^2}{2 \pi h} = E \frac{J r}{2 \beta}$$



## Conclusions on the new rf constraint



- All (?) available results of the high gradient rf tests has been collected and analyzed
- A model of the breakdown trigger has been developed based on the pulsed heating of the potential breakdown site by the field emission currents
- A new field quantity, modified Poynting vector:  $S_c$ , has been derived which takes into account both active and reactive power flow
- This new field quantity describes both travelling wave and standing wave accelerating structure experimental results rather well.
- The value of  $S_c$  achieved in the experiments agrees well with analytical estimate



## Effective pulse length for breakdown

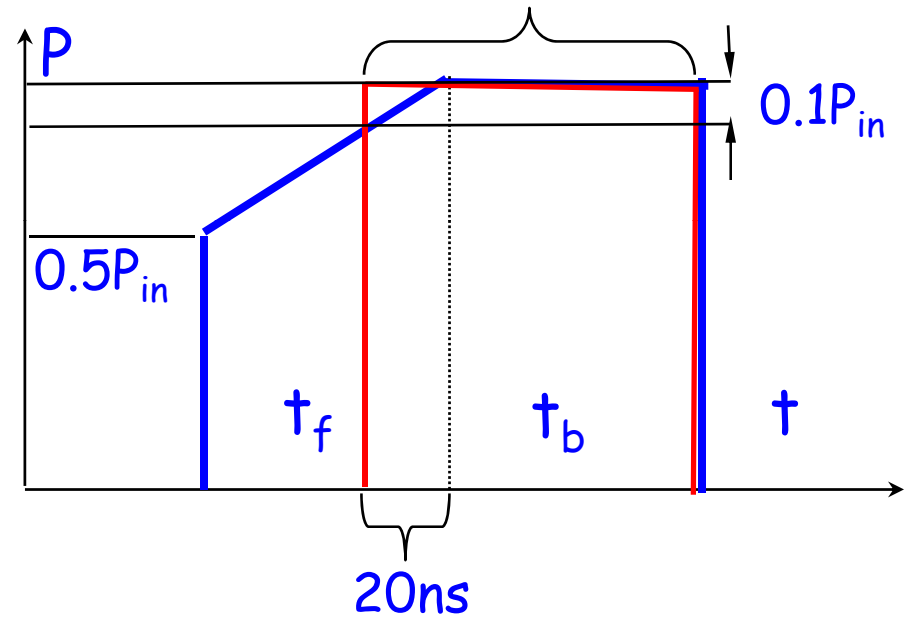
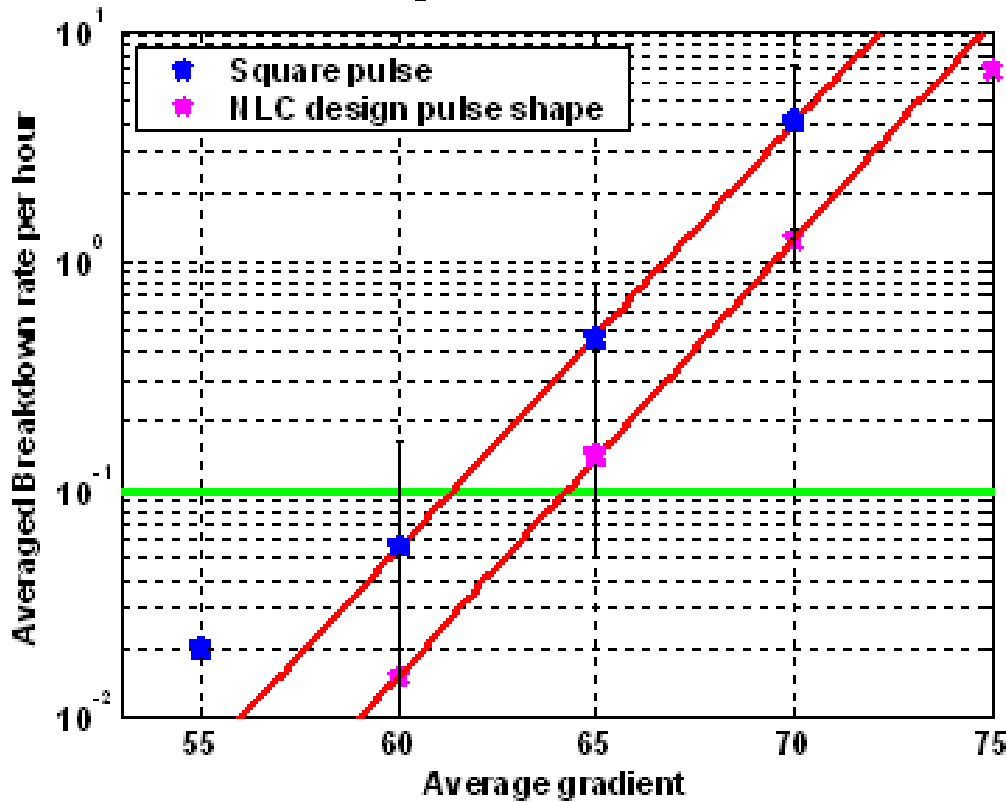


Rect-pulse => NLC-pulse  
 65 MV/m => 67.5 MV/m

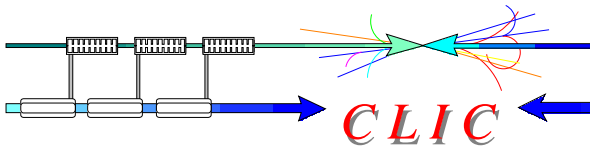
Assuming:  $E_a * t_p^{1/6} = \text{const}$   
 400ns => 320ns

### Structure Performance plots

Averaged over all structures



NLC:  $t_f = 100 \text{ ns}$ ;  $t_b = 300 \text{ ns}$

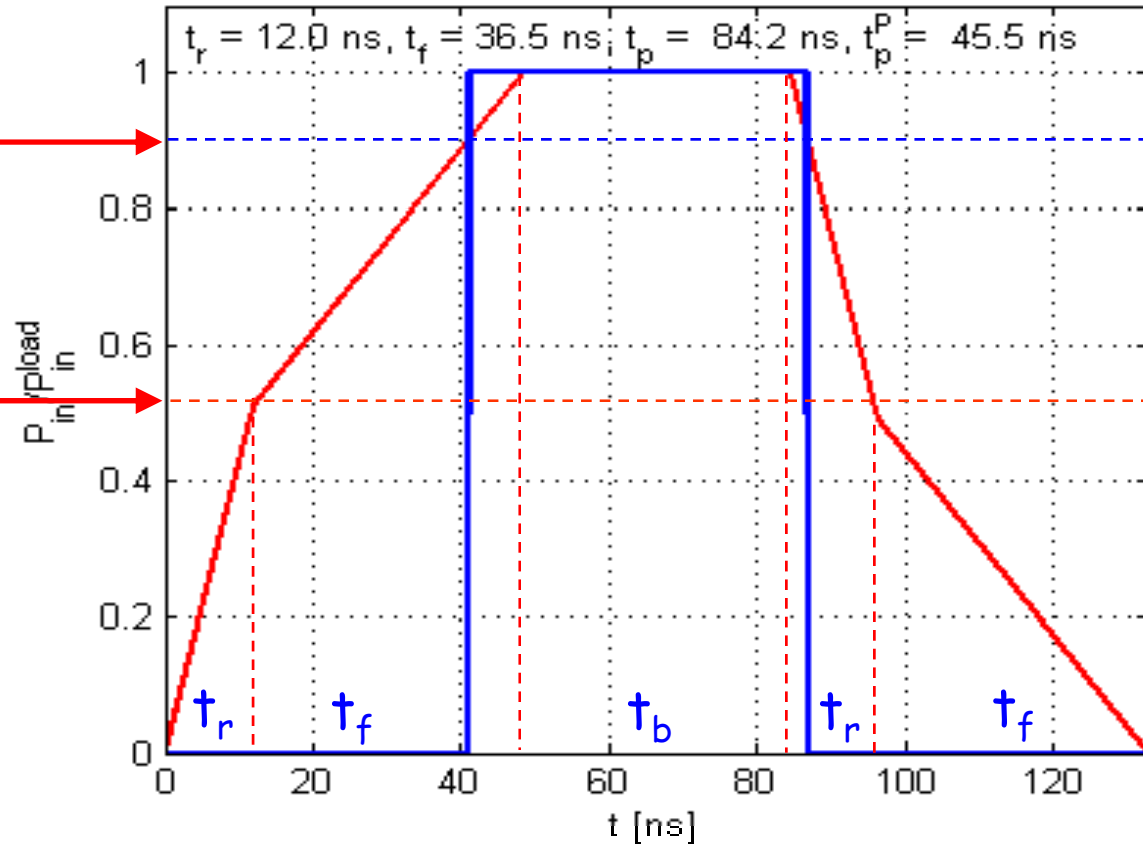


# Pulse shape dependences



$$P_{in}/P_{in}^{load} = 0.9$$

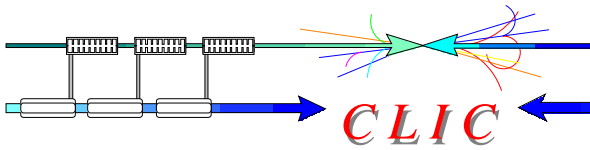
$$p_l = P_{out}^{load}/P_{out}^{unload}$$



$$\eta: t_p = t_b + t_f + t_r$$

$$\Delta T \sim (t_p^T)^{1/2}: t_p^T = t_p - [t_f \cdot (1-p_l)/2 + t_r \cdot (1-p_l/2)]$$

$$P/C^*(t_p^P)^{1/3}: t_p^P = \text{time when } P_{in}/P_{in}^{load} > 0.9 = P_{th}$$



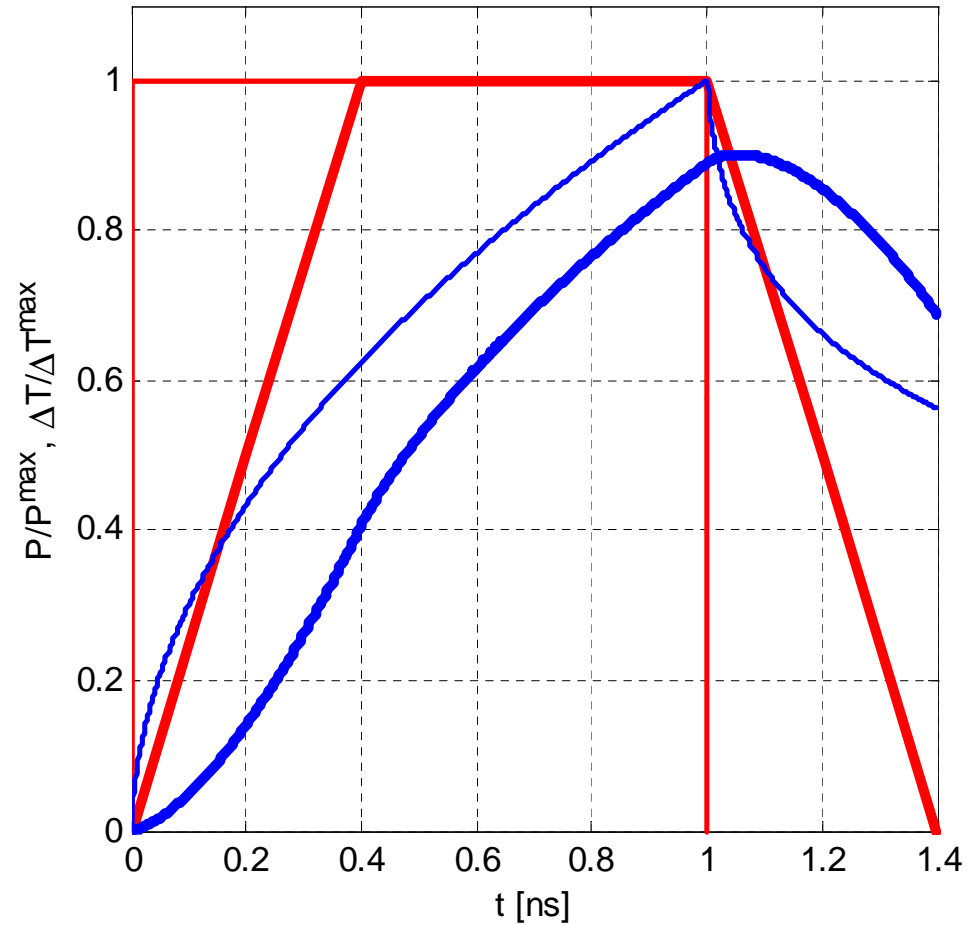
# Pulsed surface heating



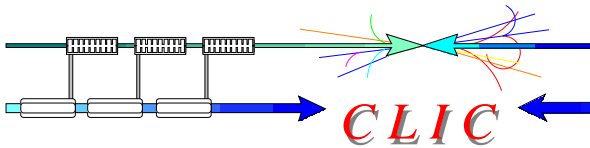
$$\Delta T(t) \sim \int_0^t \frac{P(t')}{\sqrt{t-t'}} dt'$$

For rect pulse:

$$\Delta T(t_p) \sim P_0 \cdot \sqrt{t_p}$$



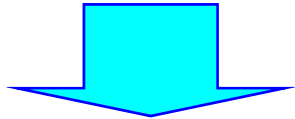




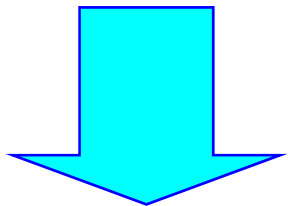
## Pulsed heating of breakdown site



BDR=const means  $\Delta T = \text{const}$

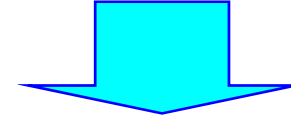


$$\Delta T(t_p) \sim P_0 \cdot \sqrt[3]{t_p}$$



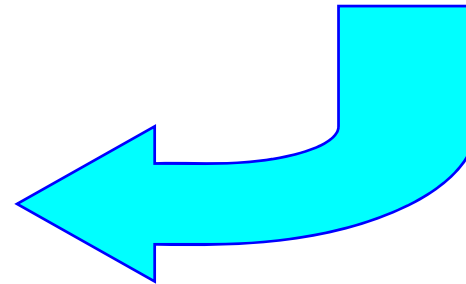
$$\Delta T_{FN}(t) \sim \int_0^t \frac{P_{FN}(t')}{(t-t')^{2/3}} dt'$$

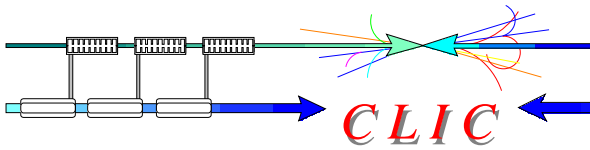
Using power loss expressed as



$$P_{FN}(t) \sim E \cdot I_{FN}$$

$$\sim E(\beta E)^2 e^{-\frac{62 \text{ GV/m}}{\beta E}}$$



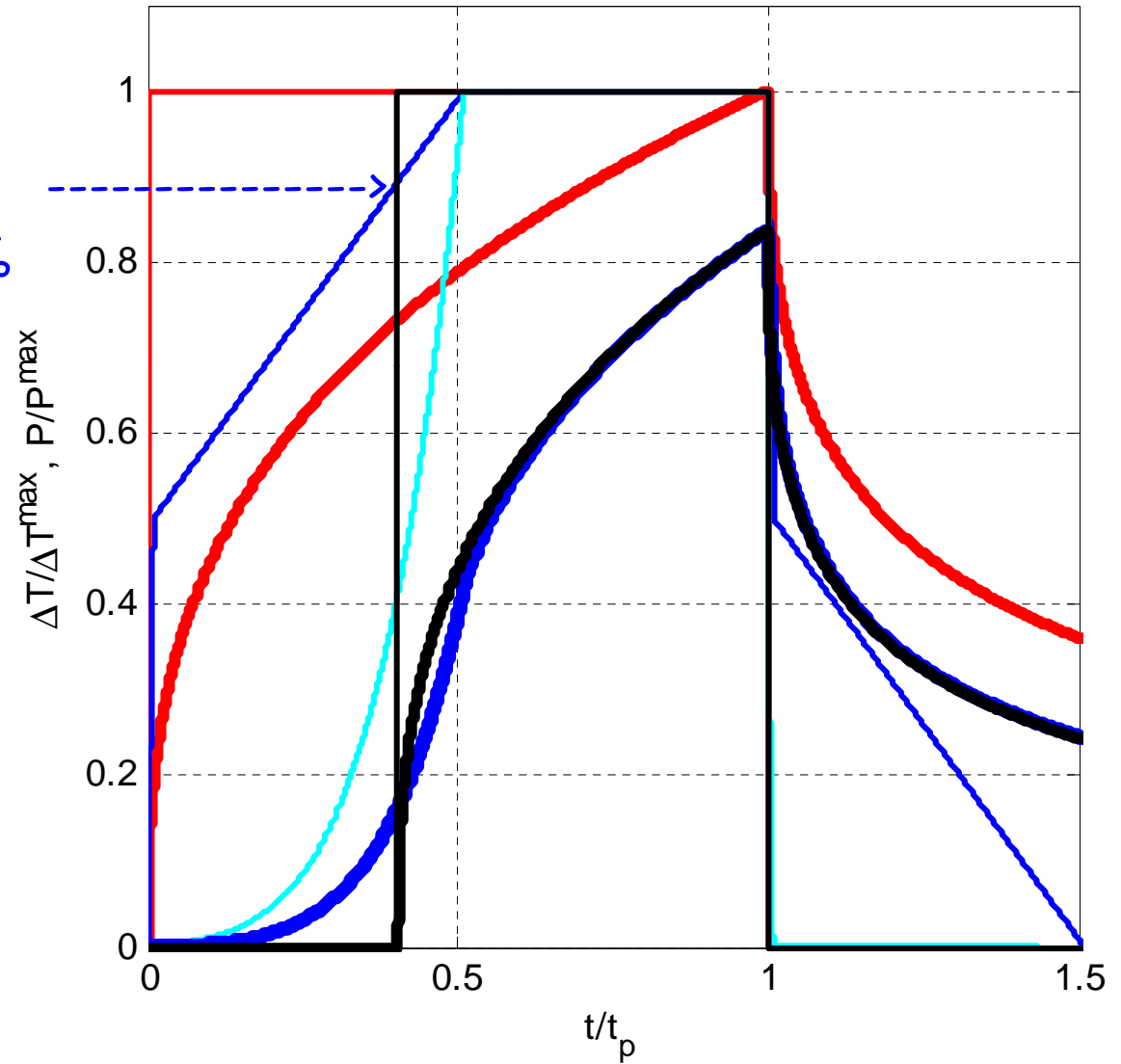


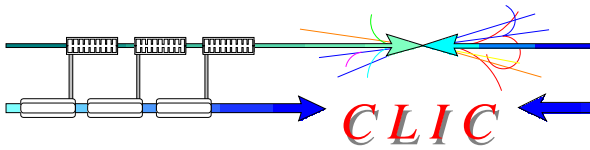
# Pulsed heating of breakdown site



## Simulation of T53vg3MC experiment

For  
 $\beta E_0 = 5 \text{ GV/m } P_{th} = 89\%$   
 $\beta E_0 = 10 \text{ GV/m } P_{th} = 84\%$

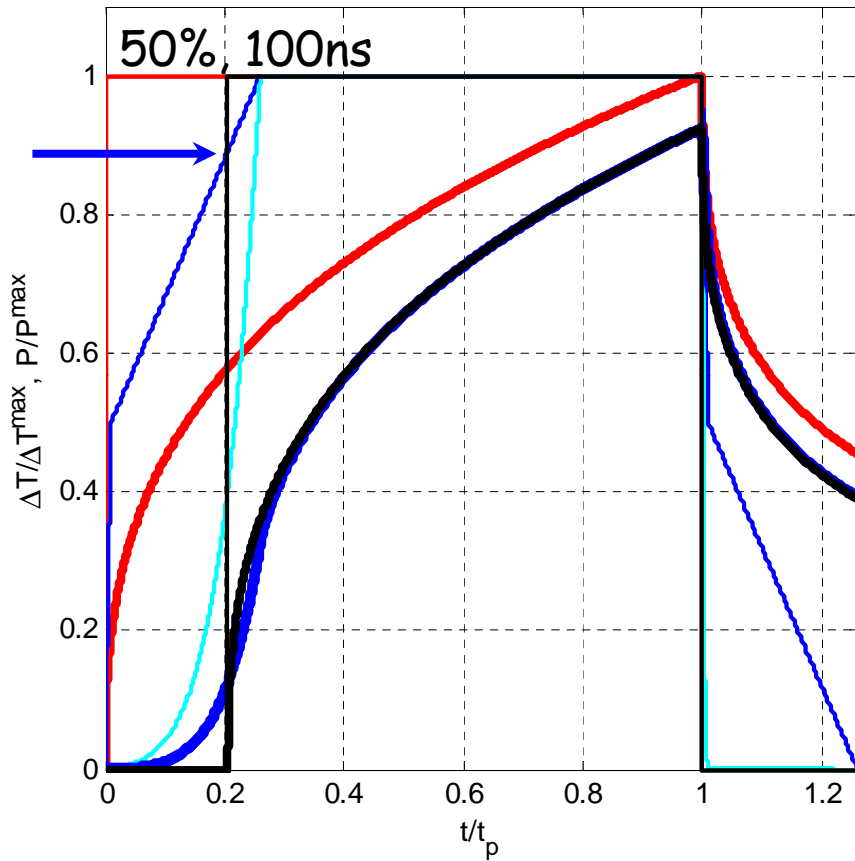




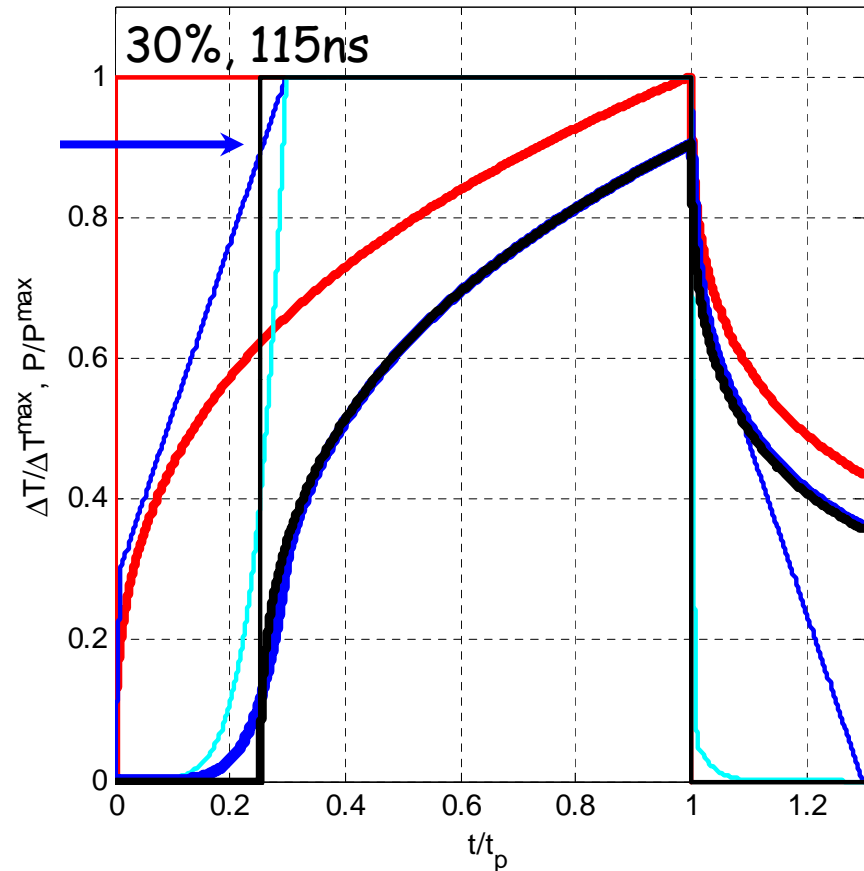
# Pulsed heating of breakdown site



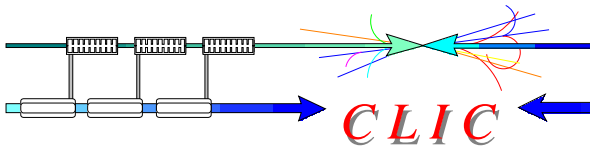
Simulation of NLC structure experiment



For  $\beta E_0 = 5 \text{ GV/m}$ ,  $P_{th} = 89\%$   
 $\beta E_0 = 10 \text{ GV/m}$ ,  $P_{th} = 84\%$



For  $\beta E_0 = 5 \text{ GV/m}$   $P_{th} = 89\%$   
 $\beta E_0 = 10 \text{ GV/m}$   $P_{th} = 83\%$



## Pulsed heating of breakdown site



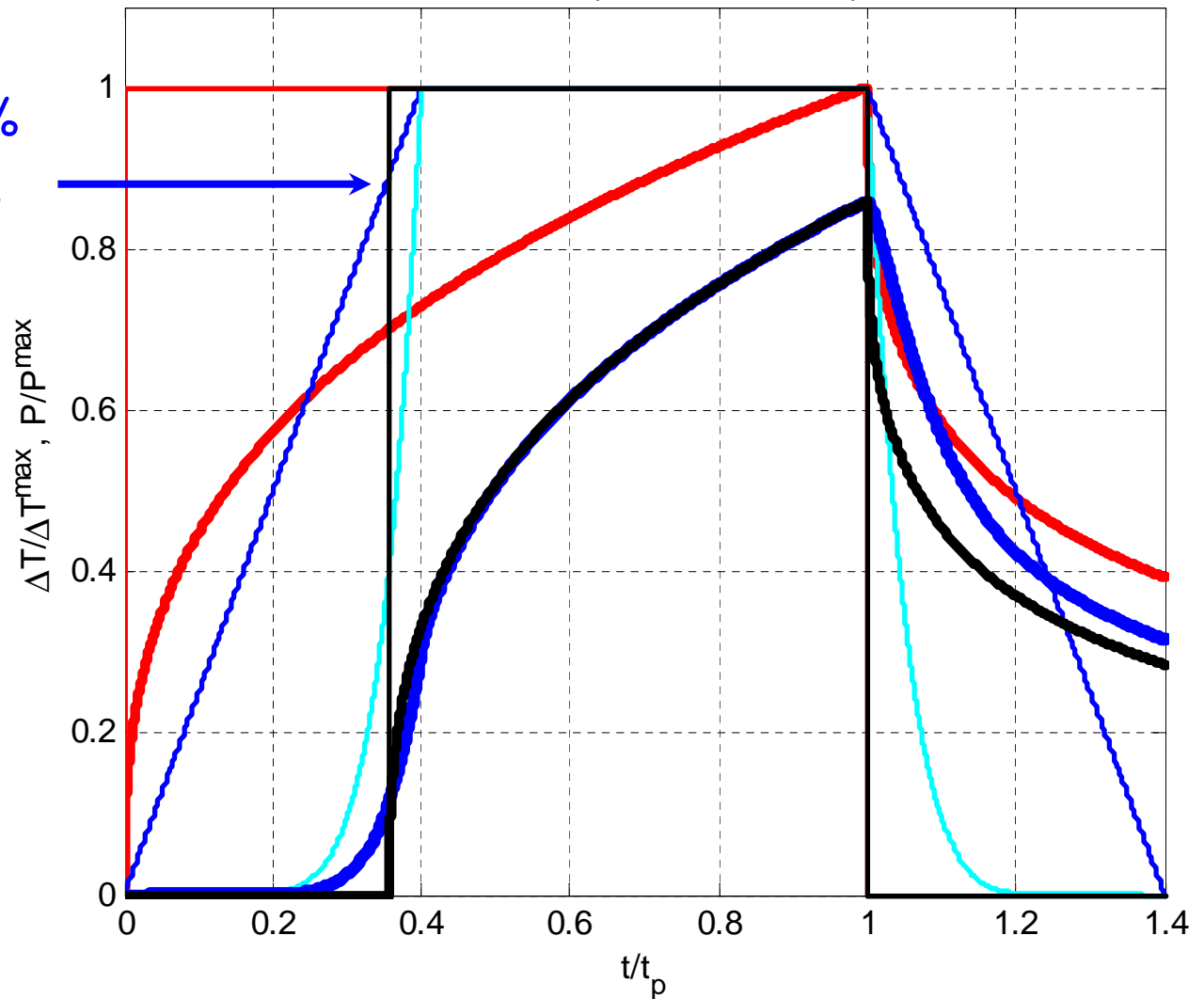
### CLIC pulse shape

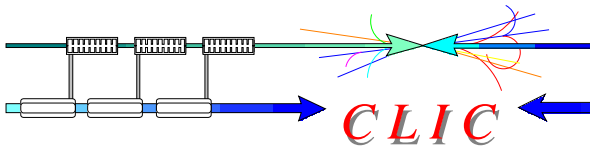
For

$$\beta E_0 = 10 \text{ GV/m } P_{th} = 83\%$$

$$\beta E_0 = 5 \text{ GV/m } P_{th} = 89\%$$

In conclusion, based on the model the threshold power level  $P_{th}$  is somewhere between 83 and 89 % of the flat top power level depending on  $\beta E_0$ .





# NLC pulse shape experiment



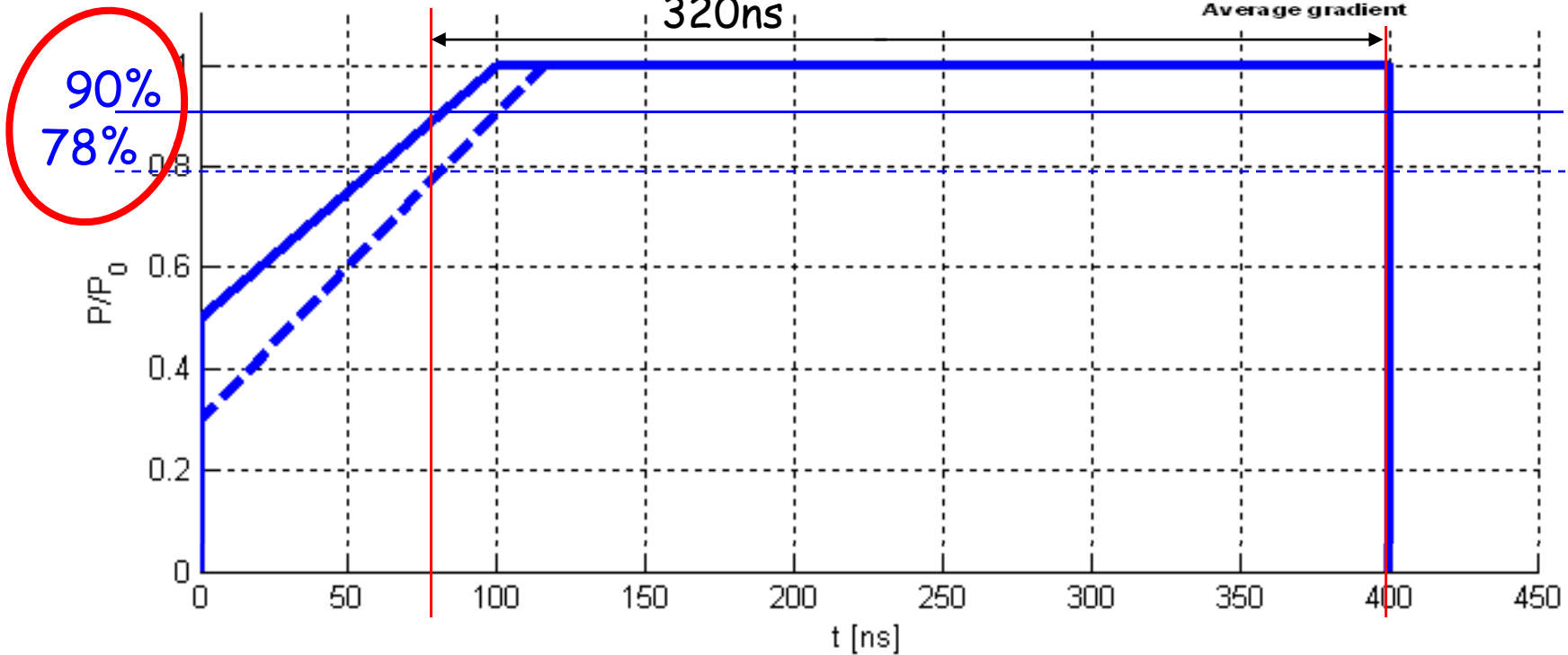
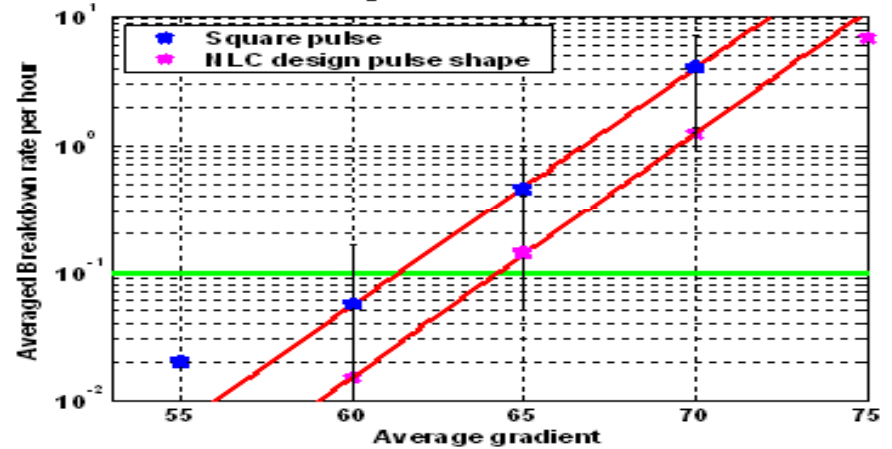
Rect.-pulse => NLC-pulse  
 $E_a^R = 65 \text{ MV/m} \Rightarrow E_a^P = 67.5 \text{ MV/m}$

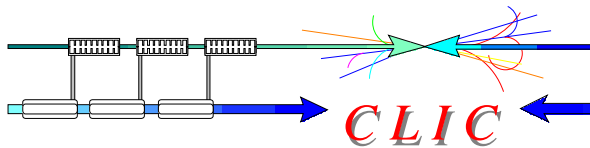
Assuming:  $E_a * t_p^{1/6} = \text{const}$

$t_p^R = 400 \text{ ns} \Rightarrow t_p^P = 320 \text{ ns}$

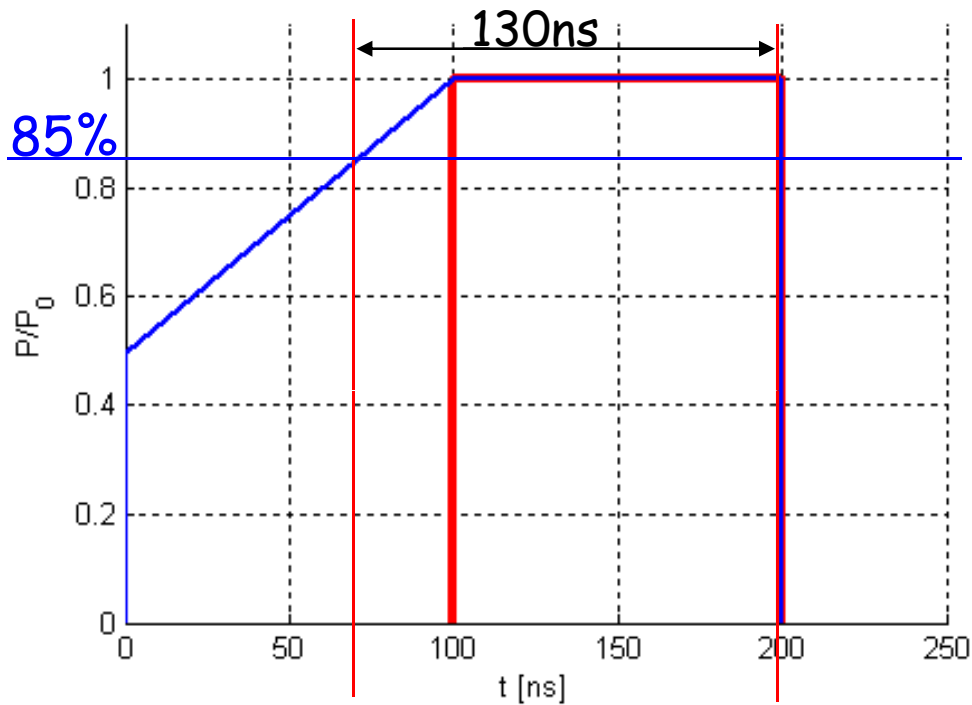
## Structure Performance plots

Averaged over all structures





## Recent experiment in T53vg3MC



At  $BDR=10^{-6}$

Effective pulse length:

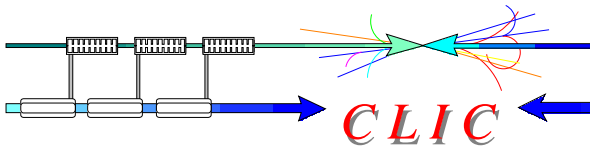
$t_p^P = 130\text{ns}$  predicted

Rect. Pulse of 100ns:

$E_a = 105\text{ MV/m}$  measured

Ramped Pulse of 100+100ns:

$E_a = 105 \cdot (100/130)^{1/3}$   
 $= 100.5\text{ MV/m}$

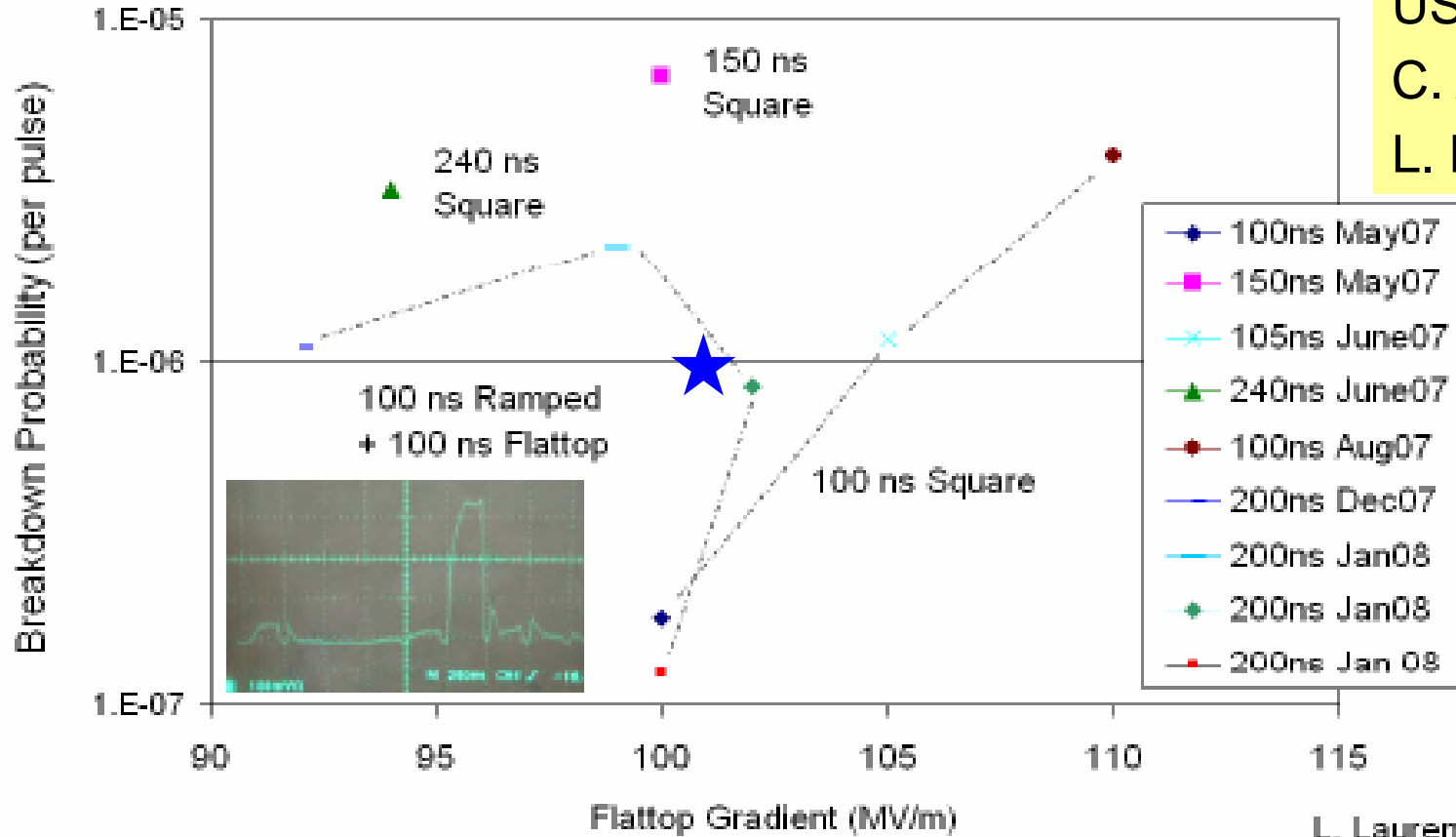


# Recent experiment on T53vg3MC

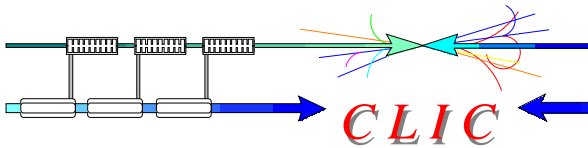


## Short Pulse Operation of T53VG3MC

USHG-2008:  
C. Adolphsen  
L. Laurent



Chris: The important point is the last (red) one where the structure ran at 100 MV/m for 70 hrs with a roughly 1e-7 bkd rate (only 2 bkds so the error is fairly large)

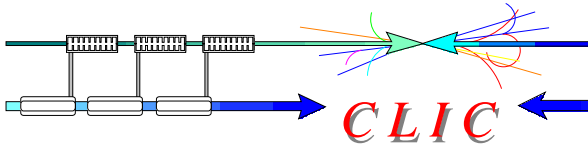


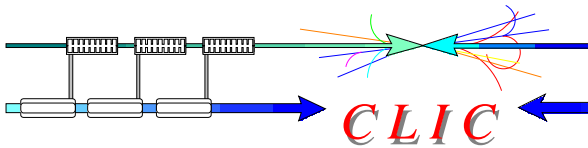
## Conclusions on pulse shape



- A theoretical model based on the pulsed heating of field emission sites has been proposed to determine the threshold power level.
- It is found that
  - $P_{th}$  varies from 89 to 83 % depending on the local electric field  $\beta E_0$ , from 5 to 10 GV/m, respectively.
  - $P_{th}$  is weakly dependent on the pulse shape (in the range of reasonable pulse shapes which can be used for acceleration)
  - It is also found that the time when power decreases from flat-top value down to threshold value does not contribute to the effective pulse length
- Modified model for effective pulse length definition is proposed. To take the flat-top time  $t_b$  plus the time when the power exceeds 85% of the flat-top level only during ramping up.
- The model predictions agree well with available experimental results on pulse shape dependence of the breakdown rate.







## Predictions for test structures



Prediction of average unloaded gradient at rect. pulse length of 100ns and BDR=1e-6 based on the results achieved in T53vg3MC: 102.3MV/m at 100ns and BDR=1e-6:

19.5Wu or  $S_c=6.2\text{MW}/\text{mm}^2@100\text{ns}$ .

	T18vg2.4	T18vg2.4	T28vg3	TD28vg3	CLIC_G
$P/C*(t_p^P)^{1/3}= 19.5Wu$					
Average unloaded gradient [MV/m]	132	128	110	104	134
$S_c=6.2\text{MW}/\text{mm}^2 @ t_p^P=100\text{ns}$					
Average unloaded gradient [MV/m]	109	106	105	103	120